GEOLOGICA CARPATHICA, JUNE 2017, 68, 3, 248–268 doi: 10.1515/geoca-2017-0018

Geochemistry, environmental and provenance study of the Middle Miocene Leitha limestones (Central Paratethys)

AHMED ALI[1,2,✉] and MICHAEL WAGREICH[2]

[1]Geology Department, Faculty of Science, Minia University, 61519 Menia, Egypt; ✉ahmad.ali@mu.edu.eg
[2]Department of Geodynamics and Sedimentology, Centre for Earth Sciences, University of Vienna, 1090 Vienna, Austria

(Manuscript received July 20, 2016; accepted in revised form March 15, 2017)

Abstract: Mineralogical, major, minor, REE and trace element analyses of rock samples were performed on Middle Miocene limestones (Leitha limestones, Badenian) collected from four localities from Austria (Mannersdorf, Wöllersdorf, Kummer and Rosenberg quarries) and the Fertőrákos quarry in Hungary. Impure to pure limestones (i.e. limited by Al_2O_3 contents above or below 0.43 wt. %) were tested to evaluate the applicability of various geochemical proxies and indices in regard to provenance and palaeoenvironmental interpretations. Pure and impure limestones from Mannersdorf and Wöllersdorf (southern Vienna Basin) show signs of detrital input (REEs=27.6±9.8 ppm, Ce anomaly=0.95±0.1 and the presence of quartz, muscovite and clay minerals in impure limestones) and diagenetic influence (low contents of, e.g., Sr=221±49 ppm, Na is not detected, Ba=15.6±8.8 ppm in pure limestones). Thus, in both limestones the reconstruction of original sedimentary palaeoenvironments by geochemistry is hampered. The Kummer and Fertőrákos (Eisenstadt–Sopron Basin) comprise pure limestones (e.g., averages Sr=571±139 ppm, Na=213±56 ppm, Ba=21±4 ppm, REEs=16±3 ppm and Ce anomaly=0.62±0.05 and composed predominantly of calcite) exhibiting negligible diagenesis. Deposition under a shallow-water, well oxygenated to intermittent dysoxic marine environment can be reconstructed. Pure to impure limestones at Rosenberg–Retznei (Styrian Basin) are affected to some extent by detrital input and volcano-siliciclastic admixture. The Leitha limestones at Rosenberg have the least diagenetic influence among the studied localities (i.e. averages Sr=1271±261 ppm, Na=315±195 ppm, Ba=32±15 ppm, REEs=9.8±4.2 ppm and Ce anomaly=0.77±0.1 and consist of calcite, minor dolomite and quartz). The siliciclastic sources are characterized by immobile elemental ratios (i.e. La/Sc and Th/Co) which apply not only for the siliciclastics, but also for marls and impure limestones. At Mannersdorf the detrital input source varies between intermediate to silicic igneous rocks, while in Kummer and Rosenberg the source is solely silicic igneous rocks. The Chemical Index of Alteration (CIA) is only applicable in the shale-contaminated impure limestones. CIA values of the Leitha limestones from Mannersdorf indicate a gradual transition from warm to temperate palaeoclimate within the limestone succession of the Badenian.

Keywords: Central Paratethys, Neogene, Leitha limestones, geochemistry, provenance.

Introduction

Sedimentary geochemistry, especially the distribution of rare earth elements (REEs) provides valuable information about marine depositional environments and sediment provenance. It is used in the assessment of the pathways of terrigenous and biogenic fluxes from the source to the sediments (Piper 1974; Elderfield & Greaves 1982; Haley et al. 2004; Anderson et al. 2007; Johannesson et al. 2014; Garbelli et al. 2016). Absolute element concentrations, relative abundance, patterns of the REEs and Ce and Eu anomalies provide guiding tools and can be used as proxies for various environmental parameters, widely applied in sedimentological studies (e.g., Elderfield 1988; Piepgras & Jacobsen 1992; Nozaki 2001; Bau et al. 2010). The absolute and relative concentrations of these elements in sediments help us to recognize, classify and unravel (1) the detrital input but also input from hydrothermal systems and related alterations; (2) the interaction with the biogeochemical cycle involving removal of elements from water bodies by adsorption and oxidation on particle surfaces and deeper regeneration within the sedimentary column; and (3) the effects of advective transport through rocks (Elderfield 1988; Kocsis et al. 2010; Azmy et al. 2011). REEs are characterized by largely similar behaviour in sediments, based on the chemical similarity as a result of the progressive filling of the inner 4f electrons orbital with increasing atomic number (de Baar et al. 1985; Nozaki 2001; Kim et al. 2012).

REEs patterns can be used to distinguish between different depositional environments. Based on the model proposed by Haley et al. (2004) three pattern types can be distinguished: (1) the linear pattern type which shows a constant, but moderate increase in the Post-Archean Australian Shale (PAAS)-normalized REEs across the series, from lower to higher atomic numbers. In this pattern type REEs are released mainly from the degradation of particulate organic matter (POC). This pattern is distinctive for oxygen levels, namely oxic and suboxic environments; (2) HREE-enrichment pattern (higher (H) atomic number REEs enriched) in which the POC source plays an important role in carrying REEs; (3) MREE bulge pattern (enrichment in middle (M) REEs) which is strongly related to high Fe-concentrations. This correlation is interpreted as a result of the dissolution of a surficial, REE-enriched solid Fe-phase which becomes the source for these REEs.

Further sediment geochemical interpretations can be performed using cerium and europium. All lanthanide elements are generally positively trivalent charged (i.e. $^{+3}$), but Ce and Eu also exist in $^{+4}$ and $^{+2}$ states, respectively. The oxidation of Ce^{+3} (loss of electron) and production of Ce^{+4} takes place trough reaction with seawater and results in the formation of cerium dioxide (CeO_2) which is highly insoluble in seawater. This criterion makes Ce a practical index for interpreting primary redox conditions in seawater using carbonates (Elderfield 1988; Bau 1991; Bau & Möller 1992; Bau & Dulski 1999; Hongo & Nozaki 2001; Dubinin 2004; Craddock et al. 2010; Schmidt et al. 2010). The reduction of Eu^{+3} to Eu^{+2} which has the ability to replace Ca^{+2} in feldspars, especially in plagioclase, is favourable in sites with submarine hydrothermal activity (Elderfield 1988) representing a secondary significant REEs source (e.g., Michard et al. 1983; Hinkley & Tatsumoto 1987; Campbell et al. 1988). There, the REEs are scavenged quickly from the hydrothermal fluids, especially Eu which is removed faster than its neighbour elements, and thus produces a positive Eu anomaly (Olivarez & Owen 1991).

In this study we analysed the mineralogy and geochemistry of Neogene limestones (Middle Miocene, Badenian Leitha limestones) at several localities in Austria and Hungary. This work deals mainly with sediment geochemistry regarding major, minor and REEs of these limestones transitional from impure to pure carbonate lithologies (distinguished by Al_2O_3 contents below or above 0.43), to get information about sediment provenance, hinterland and depositional environments. Provenance and environmental sediment geochemistry signals are distinguished and evaluated for significance in a relatively straightforward carbonate setting of the Central Paratethys Sea to test the applicability of various methods in sediment geochemistry on shallow-water carbonates in general.

Geological settings

The Vienna Basin was formed mainly as a pull-apart basin along strike-slip and normal faults due to transtension along the junction of the Eastern Alps and Western Carpathians (Royden 1985; Wessely 2006). Subsidence took place during the late Early to Middle Miocene, and led to faulting along the basin margins. Subsidence rates strongly varied during basin development with increasing rates during the early Badenian in the southern part of the basin (Wessely 1983; Lankreijer et al. 1995; Wagreich & Schmid 2002; Lee & Wagreich 2017). Islands, shoals, and small carbonate platforms were widespread in the Vienna Basin during the Middle Miocene (Dullo 1983; Riegl & Piller 2000; Schmid et al. 2001; Kováč et al. 2007; Harzhauser & Piller 2010). The Leitha Mountains (southern part of Vienna Basin), type area of the Leitha limestones, represented a shallow carbonate platform with extensive carbonate production (Schmid et al. 2001; Strauss et al. 2006). According to Riegl & Piller (2000) these Leitha limestones were deposited in a gently sloping, shallow subtidal environment.

The Eisenstadt-Sopron Basin formed a small satellite basin of the Vienna Basin to the southeast, similar in many respects also to the larger Styrian Basin (e.g., Ebner & Sachsenhofer 1995) in the south of Austria, both at the junction to the Pannonian Basin system, and having similar Leitha limestones deposits in shoaling parts of the basins. The Styrian Basin opened in the Early Miocene during the final stage of the Alpine orogeny (Ebner & Sachsenhofer 1995), and was divided by the N–S Middle Styrian Hills into the Eastern and Western Styrian subbasins (Kröll 1988). Basin subsidence during the Karpatian was a result of extensional tectonics and led to marine flooding (Ebner & Sachsenhofer 1995); eruptive volcanism accompanying the tectonic activity continued in the Badenian (Balogh et al. 1994; Slapansky et al. 1999; Seghedi & Downes 2011).

Middle Miocene shallow-water limestones in Central Europe are termed the Leitha limestones, a classical name that was already used during the 19th century (e.g., Suess 1860). Lateron, the stratigraphic unit was defined by Papp & Steininger in more detail (in Papp et al. 1978), although this definition does not conform to modern stratigraphic codes (Hedberg 1976; Salvador 1994; Steininger & Piller 1999) — as a consequence the term is not defined formally, and we use the term Leitha limestone as an informal name throughout the following paper. Leitha limestone thus refers to Middle Miocene shallow-water carbonate units composed mainly of corallinacean algae and subordinate coral-bearing strata. The latter were defined originally as being reefs (Papp et al. 1978; Dullo 1983; Tollmann 1985), but later investigations (Piller & Kleemann 1991; Piller et al. 1996, 1997; Riegl & Piller 2000) confirmed that these carbonates are not reefal deposits *sensu stricto* but rather coral carpets such as at the type locality in the Leitha Mountains of eastern Austria (Riegl & Piller 2000).

The unit is dated mainly to the Badenian (regional Central Paratethys Middle Miocene stage) which is equivalent to the Langhian–early Serravallian stages (Piller et al. 2007; Hohenegger et al. 2014). The existence of the lost Paratethys Sea was already proposed by Laskarev (1924) due to its different biogeographic entity compared to the Mediterranean Neogene. The Paratethys was subdivided into three palaeogeographic and geotectonic units, the Western, Central and Eastern Paratethys, respectively. The Eastern Alpine-Carpathian Foreland basins, from Lower Austria to Moldavia, the study area of the Vienna, Eisenstadt and Styrian basins in Austria, and the adjacent large Pannonian Basin System were included into the Central Paratethys (Piller et al. 2007).

Although a huge amount of palaeontological data is available for these Miocene limestones (e.g. Riegl & Piller 2000; Schmid et al. 2001), the exact chronostratigraphic position of individual units of Leitha limestones remains hard to unravel. In general, mostly a middle to late Badenian (Langhian to early Serravalian) age was deciphered more recently (e.g., Reuter et al. 2012; Wiedl et al. 2012, 2013, 2014; Hohenegger et al. 2014). Numerical ages for the Badenian are rare; tuffs intercalated with Leitha limestones in the Styrian basin at Retznei quarry were dated using $^{40}Ar/^{39}Ar$ method on biotite,

and yielded an age of 14.21±0.07 Ma, together with three sanidine crystals of 14.34±0.12 Ma (Handler et al. 2006). Hohenegger et al. (2009) and Hohenegger & Wagreich (2012), using cyclostratigraphy and astrochronology on combined outcrops and core data of the Badenian type locality in the southern Vienna Basin, dated the middle Badenian to 14.22 to 13.98 Ma (see also Hohenegger et al. 2014). Strauss et al. (2006) used 3D seismic reflection data, well-drill data, surface outcrops and refined biostratigraphy in the interpretation of sequence stratigraphic framework for the southern and central Vienna Basin. Three Badenian 3rd order depositional cycles, also recognized in the Styrian Basin (Schreilechner & Sachsenhofer 2007), are correlated with the TB2.3., TB2.4. and TB2.5. cycles from the global sea-level charts of Haq et al. (1987) with most Leitha limestones corresponding to the TB2.4 and TB2.5 sequences, starting at 14.8 Ma and 13.6 Ma, respectively (Hohenegger et al. 2014).

Sedimentary facies of Leitha limestones were investigated from many localities in Austria such as the type-locality at Fenk quarry (Grosshoeflein, Leitha Mts., Burgenland province, Austria, Fig. 1), where a sequence of ten coral intervals was observed (Riegl & Piller 2000). According to the authors these coral intervals represent a sequence of coral carpets and non-frame building coral communities.

Studied areas

Mannersdorf quarry (samples are denoted by M14/n, where n is sample number) is an active quarry of the Lafarge Zementwerke GmbH close to the village Mannersdorf in Lower Austria (Fig. 1), in the SW marginal part of the Vienna Basin. The quarry is located in the NE marginal part of the Leitha Mountains (Fig. 1) extends in NE–SW direction, and the mining activity continues in a SW direction. The Leitha limestones overlie mainly Middle Triassic dolostone and in some parts there is a deepening upward (transgressive) succession preserved, represented by basal breccias — gravel/conglomerate–sandstone–limestone (Fig. 2). In the NE part of the quarry a gravel layer underlies the limestones, described by Wiedl et al. (2012) as well rounded, poorly sorted, and composed of granite, quartz and dolostone pebbles and fine quartz sand. Detailed stratigraphy and facies description were given by Wiedl et al. (2012); the facies types determined by these authors will be also used in our study. Besides cross-bedded gravel facies, basal breccia facies and rhodolith facies, the bioclastic corallinacean facies include seven subfacies (i.e. Acervulina-rhodolite, Mollusc, Amphistegina, Bryozoan, Coral debris, Pholadomya and Pinna subfacies) (Wiedl et al. 2012).

The abandoned Wöllersdorf quarry area (samples are denoted by WÖ/n) is situated on the western margin of the Vienna Basin (Fig. 1). Here, Miocene sediments transgress mainly Triassic carbonates of the Northern Calcareous Alps. Several metres of Leitha limestones yield abundant Corallinacea, and molluscs (Wessely 2006). Mainly algal rudstones, grainstones and packstones were described from this area (Rohatsch 2005).

The Kummer quarry (samples are denoted by SK/n) is located 2 km to the East of St. Margarethen village in Burgenland, Austria (Fig. 2), within the Eisenstadt–Sopron Basin. The basin is surrounded by the Leitha Mountains to the North, Fertőrákos–Ruster Hügelland to the East, the Sopron Hills to

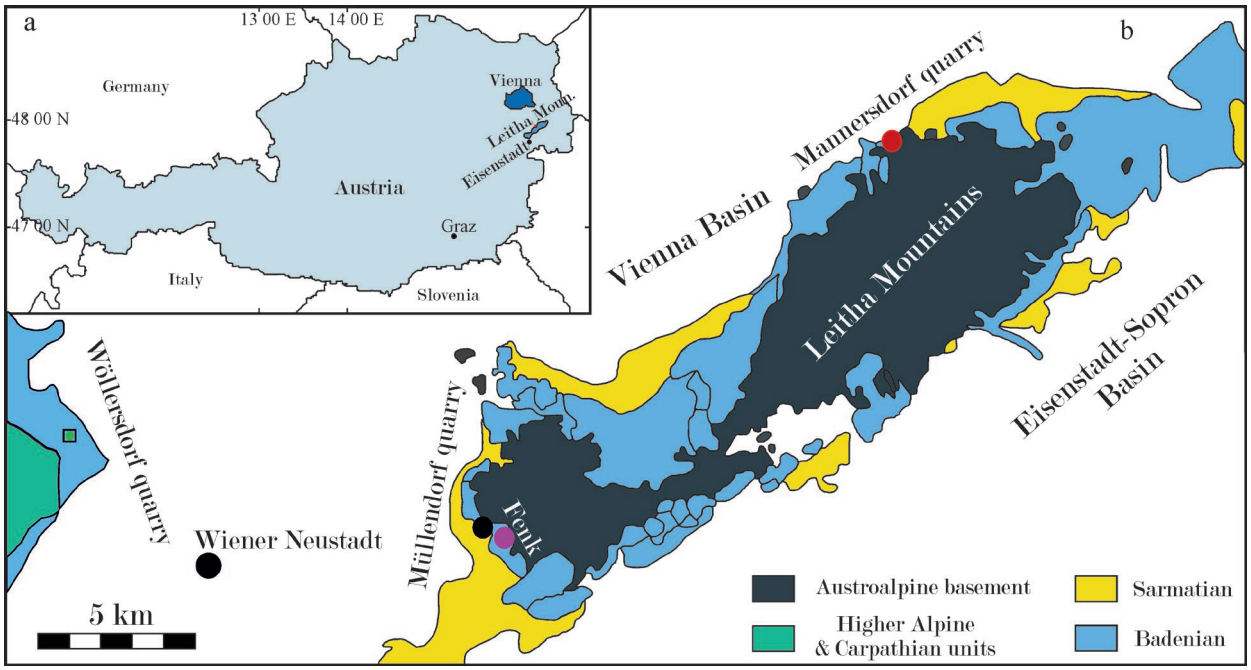

Fig. 1. a — General map of Austria with Leitha mountains location; **b** — geological map of the Leitha mountains and the southern Vienna Basin, including Leitha limestones distribution (after Strauss et al. 2006).

the South and Rosalia mountains to the West. The Leitha limestones overly Neogene gravels and Austroalpine basement rocks. In the current paper we are following the sedimentology and stratigraphy of the quarry provided by Schmid et al. (2001) who defined three sedimentary facies (i.e. corallinacean debris facies, laminated marl facies and rudstones facies) from the quarry (Fig. 2).

Fertőrákos quarry (samples are denoted by F/n) is located to the south of Kummer quarry in Hungary and has a largely similar geological setting and stratigraphy as Kummer quarry, being also part of the Eisenstadt–Sopron Basin (Fig. 2).

Rosenberg quarry (samples are denoted by RR/n) (40 km south of Graz, Fig. 3) is part of the Retznei cement quarries of the Lafarge Zementwerke GmbH in the Styrian Basin. The Leitha limestones in the area are correlated with the second Badenian transgression into the Central Paratethys which corresponds to TB 2.4 of the global sea level of Haq et al. 1987; see also Strauss et al. (2006). The stratigraphy of the studied locality shows a mixture of carbonates with silici-volcaniclastic sediments which were investigated and facies types were determined by Reuter et al. (2012). Four depositional units and six facies types (reef facies, inter-reef facies, coralline algal debris facies, rhodolith-*Porites* facies, quartz sand-*Planostegina* facies and coral carpet facies) are reported from the mixed silici-volcaniclastic succession at the Rosenberg quarry (Reuter et al. 2012).

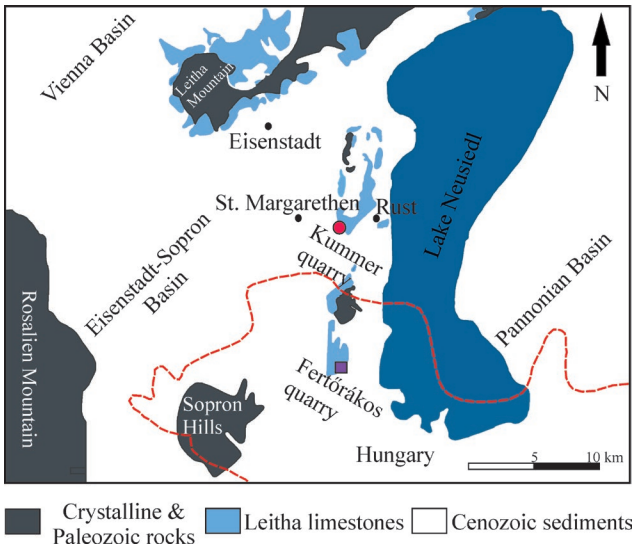

Fig. 2. Simplified geological map of the Eisenstadt–Sopron Basin, SE Vienna Basin and westernmost Pannonian Basin with location of Kummer and Fertőrákos quarries (after Schmid et al. 2001).

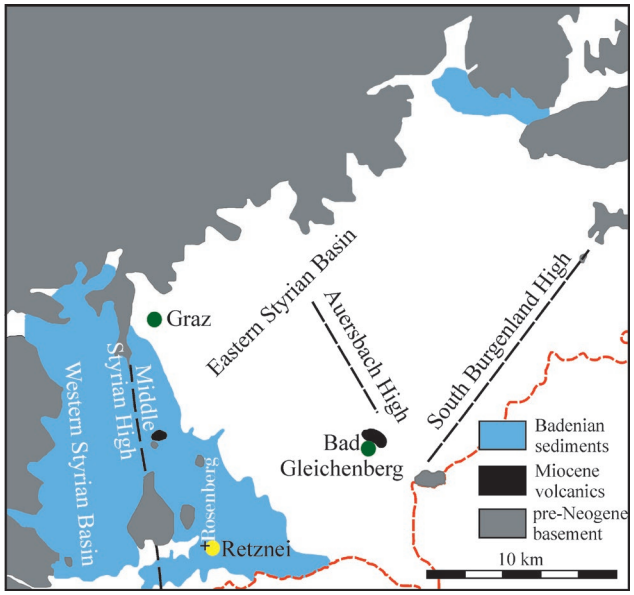

Fig. 3. Geological map of the Styrian Basin with location of the studied Rosenberg quarry near Retznei village (after Reuter et al. 2012).

Methods

In total, 91 sediment samples were collected. The 41 samples from Mannersdorf include eight clastic samples for deciphering siliciclastic background values (i.e. one sand, one conglomerate, one sandstone and five intercalated clay samples) and 33 samples represent various Leitha limestones facies types. Six Leitha limestone samples were collected at the Wöllersdorf quarry. A total of thirty samples were taken from Kummer quarry near St. Margarethen village including twenty-three limestone samples, four marly facies and three clastic samples. Eleven samples were collected at Rosenberg quarry, two from the lower siliciclastics, four samples represent limestones, one tuff sample and four upper siliciclastics samples. Only three limestone samples were taken from the Fertőrákos locality. Limestone samples include both pure and impure limestones featuring visible siliciclastic contamination.

Rock samples were cut into 5×5 cm slabs for thin sections, while all samples were powdered for X-Ray Diffraction (XRD) and whole rock geochemical analyses. The thin sections were investigated microscopically and photomicrographs were taken by Leica microscope (Leica DM2700P) with Leica camera (Leica MC170 HD) connected to computer software (LAS v4.4.0). For XRD analysis the powdered samples were analysed with a Panalytical PW 3040/60 X'Pert PRO diffractometer (CuKα radiation, 40 kV, 40 mA, step size 0.0167, 5 s per step). The X-ray diffraction patterns were interpreted using the Panalytical software "X´Pert High score plus" at the University of Vienna, Austria. SEM pictures were taken using a FEI Scanning Electron Microscope at the University of Vienna, Austria. The apparatus is equipped with secondary electron detectors for operation at high vacuum and low vacuum, as well as a back scattered electron detector and an energy dispersive X-ray detection unit (EDAX Apollo XV).

The chemical bulk rock analyses including major oxides, some minor elements (see Tables 1, 2 & 3) and loss on ignition (LOI) were detected by ICP-emission spectroscopy by AcmeLabs (Acme Analytical Laboratories Ltd., www.acmelab.com; now Bureau Veritas Mineral Labs) in Vancouver (Canada). For the analysis of trace elements (REE

and base metals) ICP-mass spectroscopy was used (www.acmelab.com). Standard deviations are mainly in the range of 0.1 to 1 % (for further details see Neuhuber et al. 2016). In addition, three samples of cements and individual shells (cement from M14/43, oyster shell from SK/28 and pectinid shell from SK/19) were selected for chemical analyses to be compared to the whole rock chemical analyses of the same samples.

The PAAS-normalized REEs patterns were obtained by dividing the measured elements by the same elements of Taylor & McLennan (1985). The PAAS value of REEs are as follows La=38, Ce=80, Pr=8.9, Nd=32, Sm=5.6, Eu=1.1, Gd=4.7, Tb=0.77, Dy=4.4, Ho=1, Er=2.9, Tm=0.4, Yb=2.8 and Lu=0.43 ppm (Taylor & McLennan 1985). Ce anomaly was quantified after the normalization of the neighbouring elements La and Pr throughout the equation (De Baar et al. 1983): Ce/Ce*=2CeN/(La+Pr)N, and the Eu anomaly was evaluated using the equation: Eu/Eu*=EuN/√SmN*GdN, where the subscript N refers to normalized value to PAAS. Sr/Ca ratio was calculated after the conversion of CaO wt. % into Ca ppm by the equation (CaO wt. %*0.7147)*10000= Ca ppm) to each sample then Ca was divided by Sr and expressed in a reverse manner where the numerator represents Sr and equals 1 and denominator represents the result of the division. These calculations were summed and averaged to all limestone samples.

Many indices were proposed to evaluate the chemical weathering such as chemical index of alteration (CIA)=$[Al_2O_3/(Al_2O_3+CaO^*+Na_2O+K_2O)]\times 100$, chemical index of weathering (CIW)=$[Al_2O_3/(Al_2O_3+CaO+Na_2O)]\times 100$ or CIW`=$[Al_2O_3/(Al_2O_3+Na_2O)]\times 100$, where CaO* represents the calcium content derived from silicates (Nesbitt & Young 1982; Harnois 1988; Chittleborough 1991; Cullers 2000). The CIA is applied here to determine the degree of chemical weathering in which CaO* is set equal to Na_2O because of the high content of calcite in all samples (McLennan et al. 1993). Mn* values were calculated by the equation [(Mn*= $Log(Mn_{sample}/Mn_{shale})/(Fe_{sample}/Fe_{shale})$ according to Wedepohl (1978) average Mn_{shale} value is 600 ppm and average Fe_{shale} value is 46150 ppm].

Results

Mineralogy

The bulk mineralogy of limestone samples from Mannersdorf examined by SEM, optical microscopy and XRD allowed the discrimination of four categories. The mineral composition of these categories is: (1) only calcite (pure limestone, Fig. 4a,b); (2) calcite and a small amount of quartz (also pure limestones); (3) calcite and a small amount of quartz and dolomite and (4) calcite, quartz and clay minerals (impure limestone, Fig. 4c,d). Besides that, the optical microscopy and Scanning Electron Microscopy (SEM) examination of the samples proved the presence of muscovite (Fig. 4a), clay minerals and feldspars with variable amounts in all studied limestones facies and sometimes pyrite and barite.

In this regard the Leitha limestones lithofacies are treated here separated in two main groups: (1) visibly "pure" limestones with minor amounts of detrital materials only confirmed by SEM and in some cases by optical microscopy, (2) "impure" limestones with variable to abundant amounts of the detritus revealed by XRD.

Samples from Wöllersdorf are subdivided into two groups according to the mineralogical composition, namely: (1) lithofacies mainly consisting of calcite, quartz and muscovite and (2) lithofacies composed of calcite, dolomite and quartz, both lithofacies are considered here as impure limestones. Limestones from the Kummer quarry display two main lithofacies: (1) limestones composed mainly of calcite and minor quartz abundance (pure limestones, Fig. 4e,f), and (2) marly facies composed of calcite with quartz and clay minerals. The Fertőrákos limestone samples are similar to the Kummer pure limestones with mainly calcite and quartz as mineral components.

The Rosenberg Leitha limestones comprise calcite, dolomite and quartz, dolomite is significantly more abundant (higher intensity peak in XRD chart, sample RR/7) in the sample directly in contact with the tuff layer, the mineralogy of the latter layer is quartz, calcite, muscovite, albite, orthoclase and gypsum.

Geochemistry

Major elements

The average chemical compositions of the Mannersdorf samples are shown in Table 1. In pure Leitha limestones samples the major oxide is CaO average of 54.98 wt. % (n=25). In contrast the lithofacies with higher clay mineral contents (impure limestones) show a gentle variation in the major oxides in which the average CaO content is lower with value of 51.56 wt. % (n=6) while average Al_2O_3 content is 1.19 wt. %.

At Wöllersdorf, the two Leitha limestones lithofacies which are impure limestones exhibit different chemical characteristics (Table 2) in which the major oxides compositions in the calcite lithofacies are dominated by CaO with an average value of 53.2 wt. % (n=3) and MgO average value is 0.64 wt. %. The limestones lithofacies with dolomite have average values of CaO=47.3 wt. % and MgO=5.7 wt. % (n=3).

At Kummer, the pure limestone lithofacies dominated by calcite have a CaO average value of 54.4 wt. % (n=23) and an average Al_2O_3=0.14 wt. %. Marly lithofacies have a lower CaO average of 46.1 wt. % (n=4), average SiO_2 of 8.7 wt. %, average Al_2O_3 of 3.2 wt. %, average Fe_2O_3 of 0.9 wt. %, while MgO; K_2O have average values of 0.8 and 0.6 wt. %, respectively. Fertőrákos Leitha limestones samples do not show differences from Kummer samples, showing that they are pure (Table 2) with a CaO average of 53.97 wt. % (n=3).

The Rosenberg Leitha limestones samples (n=4) show differences in chemical compositions with respect to their strati-

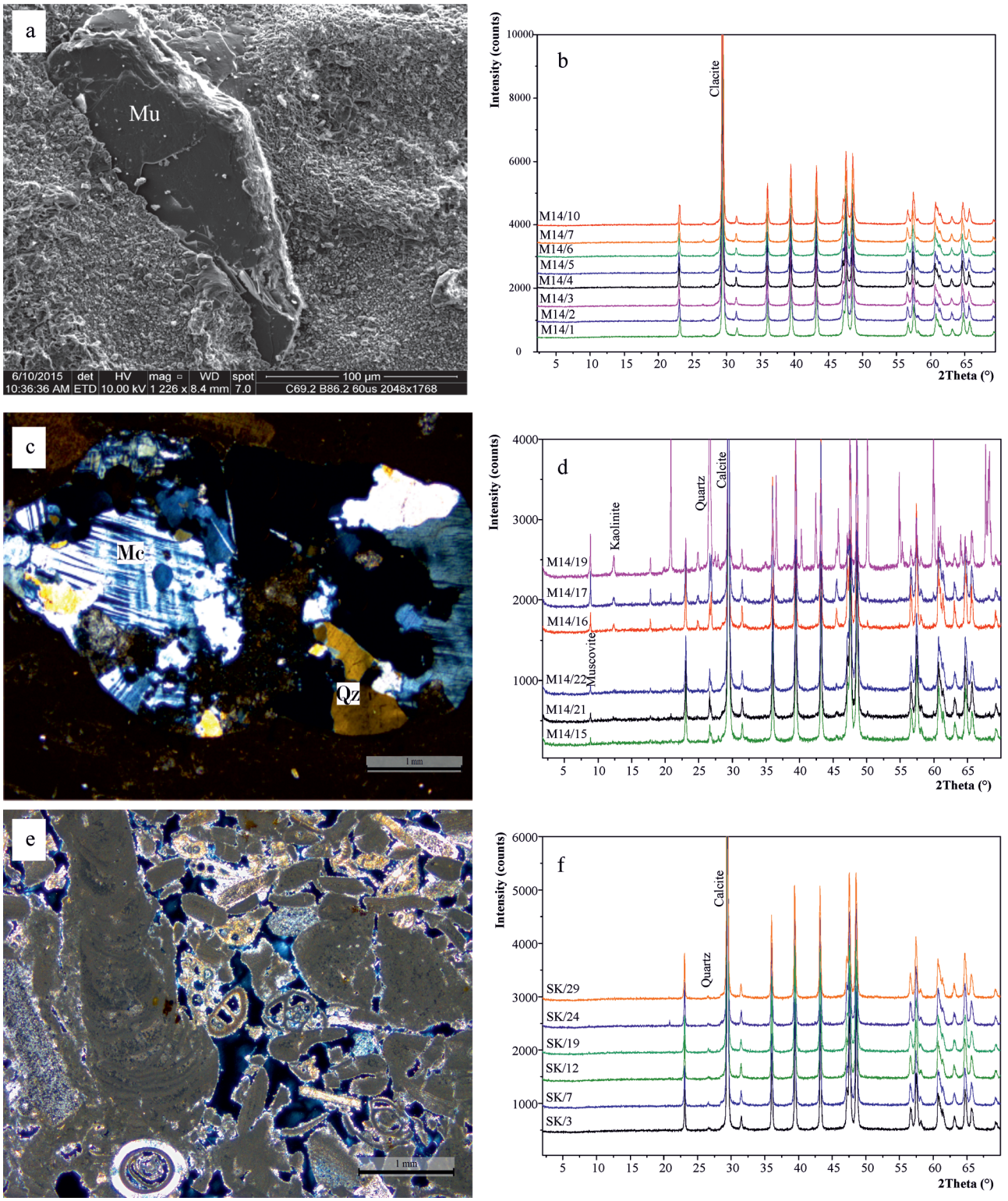

Fig. 4. Mineralogy of Leitha limestones: **a** — SEM image of pure limestone with the existence of muscovite (Mu), M14/3; **b** — XRD diagram of pure limestone from Mannersdorf; **c** — photomicrograph of impure limestone with a lithoclast composed mainly of microcline (Mc) and quartz (Qz), M14/21; **d** — XRD diagram of impure limestone from Mannersdorf; **e** — photomicrograph of pure limestone from Kummer, SK/1; **f** — XRD diagram of representative samples of pure limestone from Kummer.

Table 1: Average chemical compositions* and standard deviations of Mannersdorf Leitha limestones facies types and siliciclastics.

Rock type	Underlying clastics n=3	Intercalated clastics n= 5	Pure limestone dominated by calcite n= 8	Pure limestone with minor quartz n= 17	Impure limestone with clay minerals n= 6	Limestone with minor dolomite n=2
SiO_2	54.46±11.6	47.2±21.8	0.34±0.21	1±0.43	3.68±1.56	0.86±0.26
Al_2O_3	5.05±2.99	13.92±5.11	0.1±0.07	0.31±0.14	1.19±0.58	0.24±0.07
Fe_2O_3	1.65±0.1	4.71±2.24	0.06±0.04	0.13±0.06	0.57±0.15	0.1±0.01
MgO	0.4±0.2	1.18±0.52	0.34±0.02	0.31±0.1	0.47±0.12	0.94±0.52
CaO	18.69±7.8	12.76±16.3	55.47±0.8	54.76±0.53	51.56±1.23	54.2±0.28
Na_2O	0.19±0.22	0.28±0.34	–	–	0.02	–
K_2O	0.81±0.52	2.25±1.05	0.02±0.01	0.05±0.03	0.21±0.11	0.03±0.01
MnO	0.02±0.01	0.05±0.04	–	–	0.05±0.03	0.01
LOI	18.27±6.89	16.3±11.7	43.59±0.66	43.34±0.27	42.1±1.1	43.5±0.14
As	24.37±6.57	80.6±39.97	1.88±0.95	2.65±1.24	10.55±6.54	3.55±1.91
Co	2.63±0.35	10.12±6.63	0.47±0.26	0.61±0.38	1.6±0.85	–
Ni	–	69.2±25.9	–	–	–	–
Cr	111.8±31.6	101± 35.4	–	–	5.7±9.1	–
V	46.3±13.2	114.6±45.3	9±3.2	15.7±2.7	23.17±6.24	18.5±3.53
Sr	367.2±424.6	138.2±55.8	279. 6±40.9	208.4±22.45	195.4±59.3	170. 5±37.3
Rb	35.37±30.17	103±56.65	0.79±0.53	2.2±1.06	7.9±4.49	1.8±0.57
Cs	12.2±15.77	12.9±7.99	0.18±0.1	0.29±0.18	1.27±0.53	0.35±0.07
Ba	222±141	610±371	10.5±2.67	18±9.69	220.5±323.4	119.5±135.1
Pb	3.67±0.7	13.66±5.7	0.51±0.2	0.76±0.37	2.23±0.5	0.6±0.14
Zr	99.7±37.7	175.3±82.5	3.35±0.65	4.68±1.69	17.75±7.75	10.15±0.35
Y	4.9±1.5	25.68±10.3	0.9±0.15	1.61±0.38	14.83±19. 55	2.1±0.28
Nb	4.17±2.28	12.36±5.21	–	0.2±0.07	0.62±0.53	–
Hf	2.53±0.75	4.74±2.08	0.1±0.5	0.15±0.08	0.47±0.23	0.1
Th	1.8±1.28	11.74±5.44	0.2±0.07	0.35±0.2	0.98±0.46	0.2
U	1.3±0.36	9.78±7.33	1.18±0.43	2.86±1.5	4.6±2.6	3.5±0.28
La	6.9±4.78	27.7±15.31	0.98±0.29	1.62±0.52	4.57±1.22	0.95±0.21
Ce	13.53±10.77	54.4±27.77	1.33 ±0.36	2.45±0.81	9.02±2.46	1.45±0.07
Pr	1.53±1.26	6.71±3.29	0.13±0.04	0.29±0.1	1.05±0.31	0.19±0.02
Nd	6.13±5.24	27.1±12.53	0.65±0.23	1.19±0.4	4.58±1.48	0.75 0.35
Sm	1.1±1.01	5.53±2.47	0.11±0.05	0.21±0.07	1±0.48	0.16±0.04
Eu	0.36±0.26	1.12±0.51	0.03±0.02	0.05±0.02	0.33±0.2	0.06±0.01
Gd	1.24±0.8	5.17±2.16	0.13±0.02	0.24±0.07	1.7±1.47	0.28±0.01
Tb	0.2±0.12	0.8±0.37	0.02±0.01	0.04±0.01	0.3±0.3	0.05±0.01
Dy	1.11±0.59	4.48±1.89	0.12±0.04	0.22±0.05	1.88±2.03	0.32
Ho	0.21±0.07	0.91±0.39	0.03±0.01	0.05±0.01	0.43±0.5	0.07±0.01
Er	0.57±0.18	2.4±1.13	0.1±0.04	0.14±0.04	1.24±1.5	0.2±0.06
Tm	0.09±0.03	0.33±0.18	0.02±0.01	0.02±0.01	0.18±0.23	0.03
Yb	0.6 6±0.17	2.13±1.13	0.08±0.04	0.12±0.03	1.16±1.52	0.17±0.01
Lu	0.11±0.03	0.33±0.17	0.02±0.01	0.02±0.01	0.2±0.25	0.03
Ce/Ce*	0.94±0.04	0.93±0.02	0. 84±0.18	0.91±0.07	0. 95±0.08	0.92
Eu/Eu*	1.38±0.16	0.98±0.1	1.56±0.76	1.05±0.22	1.16±0.17	1.13±0.09
ΣREEs	33.74±24.76	139.1±68.9	3.59±0.93	6.65±1.98	27.61±9.79	4.7±0.18
$(La/Yb)_N$	0.74±0.42	0.94±0.07	0.92±0.39	0.99±0.2	0.65±0.41	0.42±0.08
Y/Ho	23.24±1.2	28.5±1.8	30.6±9.4	36.7±11.6	33.2±7.4	30.2±2.1

* oxides in wt. %, elements in ppm and (–) indicates not detected

graphic position within the Leitha limestone interval. Two samples were collected from the lower and upper parts of the main limestone bank (Reutel et al. 2012), in contact to underlaying and overlaying siliciclastics, and two samples from the middle portion of the bank (Table 3). In the former ones the average CaO is 51.46 wt. % and Al_2O_3 average is 0.75 wt. %. The latter samples have higher CaO with average of 55.12 wt. % and lower Al_2O_3 average of 0.06 wt. %. The tuff layer (sample RR/6) has the lowest SiO_2 content among the sampled siliciclastics with 16.93 wt. % and the highest content of MgO with 8.31 wt. %. The CaO, Al_2O_3, Fe_2O_3 and K_2O contents are 29.91, 5.73, 3.57 and 1.26 wt. %, respectively.

Minor elements

Minor element contents in the Mannersdorf samples are low in the limestone facies compared to the siliciclastics (Table 1). The only exception is strontium (Sr) which has a significantly higher content in the limestone facies. The average Sr content in the different limestone facies varies from pure (221 ppm, n= 25) to impure limestones (224 ppm, n=6) at Mannersdorf, recording Sr/Ca ratios with an average of 1/1845. Interestingly, the arsenic (As) content in siliciclastic samples is variable and ranges from low (9.6 ppm) to high (136.6 ppm) contents. In contrast As content in the limestones is considerably lower.

Table 2: Average chemical compositions* and standard deviations of Wöllersdorf, Kummer and Fertőrákos Leitha limestones facies types and Kummer siliciclastics.

Rock type	Wöllersdorf impure limestones with clays n=3	Wöllersdorf impure limestones with dolomite n=3	Kummer pure limestones n= 23	Kummer marls n= 4	Kummer siliciclastics n=3	Fertőrákos pure limestones n= 3
SiO_2	2.38±1.46	2.96±1.45	0.61±0.2	8.7±1.53	26.73±9.02	1.78±0.44
Al_2O_3	0.75±0.41	0.52±0.13	0.14±0.06	3.18±0.48	9.12±2.59	0.27±0.08
Fe_2O_3	0.21±0.1	0.22±0.05	0.28±0.17	0.9±0.2	3.26±2.06	0.09±0.01
MgO	0.64±0.01	4.7±2.9	0.61±0.06	0.75±0.12	1.69±0.3	0.57±0.03
CaO	53.21±1.31	47.26 ±4.38	54.35±0.45	46.11±1.18	27.81±9.11	53.97±0.31
Na_2O	0.01	0.01	0.03±0.01	0.04±0.01	0.1±0.02	0.08±0.03
K_2O	0.13±0.07	0.1±0.03	0.03±0.01	0.56±0.07	1.61±0.46	0.0.3±0.01
MnO	–	–	0.06±0.05	0.13±0.14	0.02±0.01	0.05±0.02
LOI	42.47±0.78	43.1±0.21	43.75±0.24	39.3±1.12	28.8±5.68	42.97±0.23
As	1.43±0.29	1.7±0.7	1.7±1.3	3±2.76	159.8±260.4	0.77±0.06
Co	0.53±0.25	0.4±0.14	0.42±0.25	0.98±0.32	6.97±5.58	0.25 ±0.15
Ni	2.93±1.27	4.03±0.32	1.99±1.45	3.08±1.08	46.87±43.89	0.83±0.4
Cr	–	–	–	25.66±6.55	68.42 ±23.7	–
V	011±0.03	0.07±0.01	11.33±5.17	30.75±2.36	94.67±40.51	15.33±5.77
Sr	253.2±15.5	141.5±24.6	570. 7±139	196.6±53.4	359.8±113.1	629±45
Rb	5.97±2.82	3.93±1.03	1.31±0.53	29.63±3.18	91.33±30.33	1.57±0.35
Cs	0.43±0.23	0.33±0.16	0.21±0.17	3.98±0.62	14.13±5.69	0.23±0.06
Ba	18±7.8	9±1	20.57±4.07	70.25±3.3	170.3±47.4	17.33±0.58
Pb	0.9±0.2	1.1±0.26	1±0.33	1.8±0.39	9.1±6.97	0.7
Zr	16.93±7.03	22.63±13.75	3.71±2.65	50.8±58.4	59.8±17.15	6.4±4.9
Y	2.6±0.72	2.77±0.59	6.15±1.15	7.7±1.2	18.57±5.74	6.2±0.4
Nb	0.8±0.46	0.37±0.21	0.25±0.07	2.2±0.59	6.6±1.9	–
Hf	0.47±0.21	0.6±0.36	0.15±0.08	1.4±1.41	1.7±0.52	–
Th	0.6±0.26	0.67±0.12	0.44±0.16	2.5±0.45	7.53±2.48	0.43±0.06
U	1.63±0.78	1.7±0.44	1.97±0.47	2.18±1.06	3.9±1.51	1.3±0.26
La	2.4±1.13	2.7±0.5	3.76±0.73	8.33±0.92	22.53±7.19	3.33±0.25
Ce	4.57±2.63	4.8±0.87	4.46±1.01	14.43±1.96	43.17±15.74	4.1±0.4
Pr	0.54±0.27	0.59±0.12	0.72±0.14	1.78±0.25	5.03±1.59	0.69±0.05
Nd	2.17±1.16	2.37±0.58	3.18±0.63	7.08±1.24	19.23±6.19	3±0.1
Sm	0.44±0.24	0.5±0.15	0.65±0.14	1.35±0.28	3.72±1.07	0.62±0.08
Eu	0.09±0.06	0.1±0.03	0.16±0.3	0.31±0.05	0.83±0.29	0.17± 0.02
Gd	0.43±0.16	0.54±0.07	0.82±0.14	1.33±0.26	3.6±1.3	0.83±0.08
Tb	0.07±0.03	0.08±0.02	0.13±0.02	0.21±0.03	0.55±0.19	0.12±0.01
Dy	0.44±0.19	0.45±0.11	0.79±0.15	1.2±0.21	3.08±1.03	0.81±0.09
Ho	0.08±0.03	0.09±0.02	0.16±0.02	0.22±0.03	0.59±0.22	0.16±0.03
Er	0.23±0.08	0.27±0.06	0.47±0.08	0.67±0.12	1.67±0.52	0.46±0.05
Tm	0.03±0.01	0.04±0.01	0.06±0.01	0.095±0.01	0.23±0.08	0.06±0.01
Yb	0.2±0.09	0.23±0.08	0.38±0.07	0.58±0.07	1.51±0.45	0.38±0.09
Lu	0.04±0.01	0.04±0.01	0.06±0.01	0.1±0.01	0.22±0.06	0.06±0.01
Ce/Ce*	0.9±0.08	0.87±0.07	0.62±0.05	0.86±0.02	0.92±0.04	0.62±0.01
Eu/Eu*	0.88±0.26	0.91±0.19	1.02±0.09	1.08±0.1	1.05±0.04	1.09±0.17
ΣREEs	11.72±6.07	12.8±2.5	15.79±2.91	37.67±5.24	106±35.9	14.8±0.98
$(La/Yb)_N$	0.88±0.04	0.9±0.14	0.74±0.1	1.06±0.03	1.1±0.04	0.66±0.13
Y/Ho	33±1.7	31±2.2	38.56±3.05	34.6±2.8	31.7±2	39±4.7

* oxides in wt. %, elements in ppm and (–) indicates not detected

In the Wöllersdorf samples the minor element concentrations are still low without major variations between the two lithofacies and similar to those from Mannersdorf quarry, except for Sr which is lower in the lithofacies containing dolomite with an average value of 141.5 ppm, with Sr/Ca ratio of 1/2412, and the other lithofacies has an average value of 253 ppm and Sr/Ca ratio of 1/1506.

In general minor elements in the Kummer samples are again low except for Sr. Unlike the Mannersdorf and Wöllersdorf samples, Sr content is higher in the Leitha limestones lithofacies with an average of 571 ppm (n=23). The Sr/Ca ratio in this locality also differs significantly from Mannersdorf and Wöllersdorf, with average value of 1/716. The average value in the intercalated marly facies is 360 ppm. The Sr content at Fertőrákos averages 629 ppm and Sr/Ca ratio of 1/613.

The Rosenberg samples show high Sr contents compared to the other localities not only in the Leitha limestones but also in surrounding siliciclastics. The average content in limestones (both pure and impure, n=4) equals 1271 ppm with Sr/Ca ratio average of 1/301, while Sr in the tuff layer has a value of 1074.1 ppm.

Table 3: Average chemical compositions* and standard deviations of Rosenberg Leitha limestones facies types and siliciclastics.

Rock type	Rosenberg lower siliciclastics n=2	Rosenberg pure limestones n=2	Rosenberg impure limestones n=2	Rosenberg tuff layer	Rosenberg upper siliciclastics n= 4
SiO_2	25±0.23	0.25±0.04	2.24±0.22	16.93	41.42±7.47
Al_2O_3	4.78±1.71	0.06±0.04	0.75±0.07	5.73	8.93±4.08
Fe_2O_3	3.06±0.35	0.06±0.03	0.35±0.01	3.57	3.88±1.34
MgO	2.42±0.04	0.64±0.07	1.81±0.93	8.31	4.17±1.32
CaO	32.96±6.33	55.1±0.54	51.4±1.3	29.91	17.86±9.05
Na_2O	0.63±0.23	0.02	0.07±0.01	0.44	0.99±0.18
K_2O	1.17±0.36	0.02±0.01	0.16±0.03	1.26	1.91±0.86
MnO	0.04	–	0.01	0.02	0.09±0.07
LOI	28.95±4.45	43.6±0.42	42.85±0.07	32.7	19.85±5.6
As	5.05±1.63	1.3±0.42	1.85±0.5	68.8	6.25±2.92
Co	7.1±2.97	0.65±0.07	1.15±0.35	4.6	10.1±5.52
Ni	20.95±5.02	0.5-	3.2±1.13	35	47.28±26.64
Cr	75.26±9.68	–	–	123.2	148.8±22.6
V	39.5±9.19	–	15±1.4	99	78±38
Sr	750±110	1378±229	1164±325	1074.1	518±360
Rb	43.1±12.3	0.8±0.28	7.1±0.42	48.5	73.1±38.5
Cs	2.5±0.28	0.2	0.6	38	4.63±2.59
Ba	187.5±105.4	20.5±2.12	43.5±13.4	206	285.3±113
Pb	6.75±3.6	0.95±0.07	1.3±0.28	25.7	7.45±4.26
Zr	68.4±11.6	1.3±0.28	8.85±0.21	78.4	137.1±56.1
Y	13.95±6.01	2.65±0.07	2.95±0.21	19.8	20.9±7.2
Nb	5.75±2.62	–	0.65±0.07	6.7	9.1±4.24
Hf	1.75±0.35	–	0.2	2	3.73±1.43
Th	4.1±1.9	–	0.7±0.14	7.4	6.08±3
U	2.6±1.6	1.2±0.71	2.25±1.77	9.5	3.28±1.23
La	14.95±6.15	1.4±0.28	3.05±0.21	18.2	22 ±9.01
Ce	29.5±12.73	1.85±0.07	5.05±0.07	37.3	43.38±18.36
Pr	3.28±1.36	0.27±0.02	0.63	4.64	5.11±2.29
Nd	12.75±6.01	1.15±0.07	2.45±0.49	18.7	19.3±9
Sm	2.58±1.36	0.22±0.01	0.48±0.08	3.79	3.99±1.83
Eu	0.62±0.28	0.08	0.12±0.02	0.86	0.86±0.35
Gd	2.64±1.3	0.26	0.49±0.04	3.7	3.67±1.51
Tb	0.41±0.18	0.06±0.01	0.08±0.01	0.57	0.6±0.28
Dy	2.34±1.2	0.29±0.01	0.45±0.01	3.16	3.55±1.31
Ho	0.47±0.18	0.07±0.01	0.1±0.01	0.62	0.7±0.24
Er	1.31±0.64	0.22±0.01	0.27±0.02	1.63	2.09±0.74
Tm	0.18±0.08	0.03±0.01	0.05±0.01	0.21	0.3±0.11
Yb	1.21±0.57	0.19±0.04	0.22±0.01	1.41	1.96±0.74
Lu	0.2±0.08	0.02	0.04±0.01	0.22	0.29±0.1
Ce/Ce*	0.96±0.02	0.7±0.08	0.84±0.04	0.93	0.94±0.01
Eu/Eu*	1.13±0.05	1.58±0.03	1.13±0.35	1.07	1.06±0.04
ΣREEs	72.42±32.14	6.09±0.33	13.44±0.29	95.01	107.8±45.6
$(La/Yb)_N$	0.93±0.13	0.54±0.01	1.04±0.04	0.95	0.83±0.17
Y/Ho	29.4±1.3	39±8.8	31±0.08	32	29.8±1.99

* oxides in wt. %, elements in ppm and (–) indicates not detected

REEs patterns

In the Mannersdorf samples the overall concentration of the REEs in the carbonate facies in general is lower and varying due to the clay content compared to the intercalated clastics with contents higher than 110 ppm. The average ΣREEs is 5.7 ppm (n=25) in the absence of clays (pure limestones) while this average is enhanced due to the presence of clays to 27.6 ppm (n=6). The total REEs value is strongly positive correlated to Al_2O_3 wt. % (r=0.95), as well as Zr (r=0.92); on the other hand, it is negatively correlated to CaO wt. % (r=−0.84). PAAS normalized REEs patterns of the intercalated clastics are flattened and show average shale patterns (Fig. 5a). PAAS (Taylor & McLennan 1985) normalized REEs patterns of limestones facies from Mannersdorf are almost flat with negative Ce anomaly in pure limestones (Fig. 5b, c) but this anomaly is less pronounced in impure limestones (Fig. 5d). The LREEs/HRREs ratio is marked by the $(La/Yb)_N$ ratio which has an average value around 1 (i.e. 0.97, n=30), apart from some samples which exhibit HREEs enrichment with an average value of 0.45 (n=9).

The total REEs content in Wöllersdorf samples averages 12.3 ppm (n=6). The PAAS normalized RREs patterns are nearly flat (Fig. 6a) with low LRREs/HRREs ratio indicated by $(La/Yb)_N$ ratio ranging from 0.74 to 0.99 with an average of 0.86.

Pure limestone facies from Kummer have PAAS normalized REEs patterns which resemble seawater patterns with negative Ce anomaly and HREEs/LREEs enrichment (Fig. 6b). The total REEs content in this facies has an average of 15.8 ppm (n=23), this content has very weak negative correlation with Zr (r=−0.05), weak positive correlation with Al_2O_3 with r=0.27 and weak negative correlation with CaO with r=−0.21. The $(La/Yb)_N$ ratio average of this facies is 0.74. The pattern shape in the marly facies is characterized by MREEs enrichment (Fig. 6c) and the REEs content is higher than in the limestones facies with average values of 37.7 ppm, as well as the $(La/Yb)_N$ ratio average of 1.1. The clastic facies has a flat pattern (Fig. 6c) with the highest concentration among the facies in Kummer, with average REEs content of 106 ppm and $(La/Yb)_N$ ratio average of 1.1. Fertőrákos pure limestones exhibit a similar REEs pattern to those from Kummer (Fig. 6d) with average content of 14.8 ppm and $(La/Yb)_N$ ratio average of 0.66.

The Rosenberg limestones show two REEs patterns: (1) for two samples in contact with siliciclastics there is a flat pattern with average 13.4 ppm and $(La/Yb)_N$ ratio average of 1.04 and a seawater like REEs pattern with pronounced Ce anomaly and REEs average content of 6.09 ppm and HREEs enrichment indicated by $(La/Yb)_N$ ratio average of 0.54 (Fig. 7a); (2) the REEs patterns of the underlying and overlying layers and the intercalated tuff layer are flat with MREEs enrichments and $(La/Yb)_N$ ratio average of 0.9 (Fig. 7b).

Ce anomaly

In Mannersdorf the values of the anomaly in the various rock types are approximately the same, the average value in pure and impure limestones is 0.9 (n=33). Samples from Wöllersdorf have Ce/Ce* values close to those of the Mannersdorf average of 0.88. The Kummer pure limestones facies has an average Ce anomaly of 0.62, while the marly facies has a higher average of 0.86 and the highest average value is recorded in the intercalated clastics where it reaches 0.92. The average Ce anomaly in limestones from Fertőrákos is also 0.62. Pure limestones from Rosenberg quarry have average Ce anomaly value of 0.7 (n= 2) while the average value of the impure facies is 0.84 (n=2).

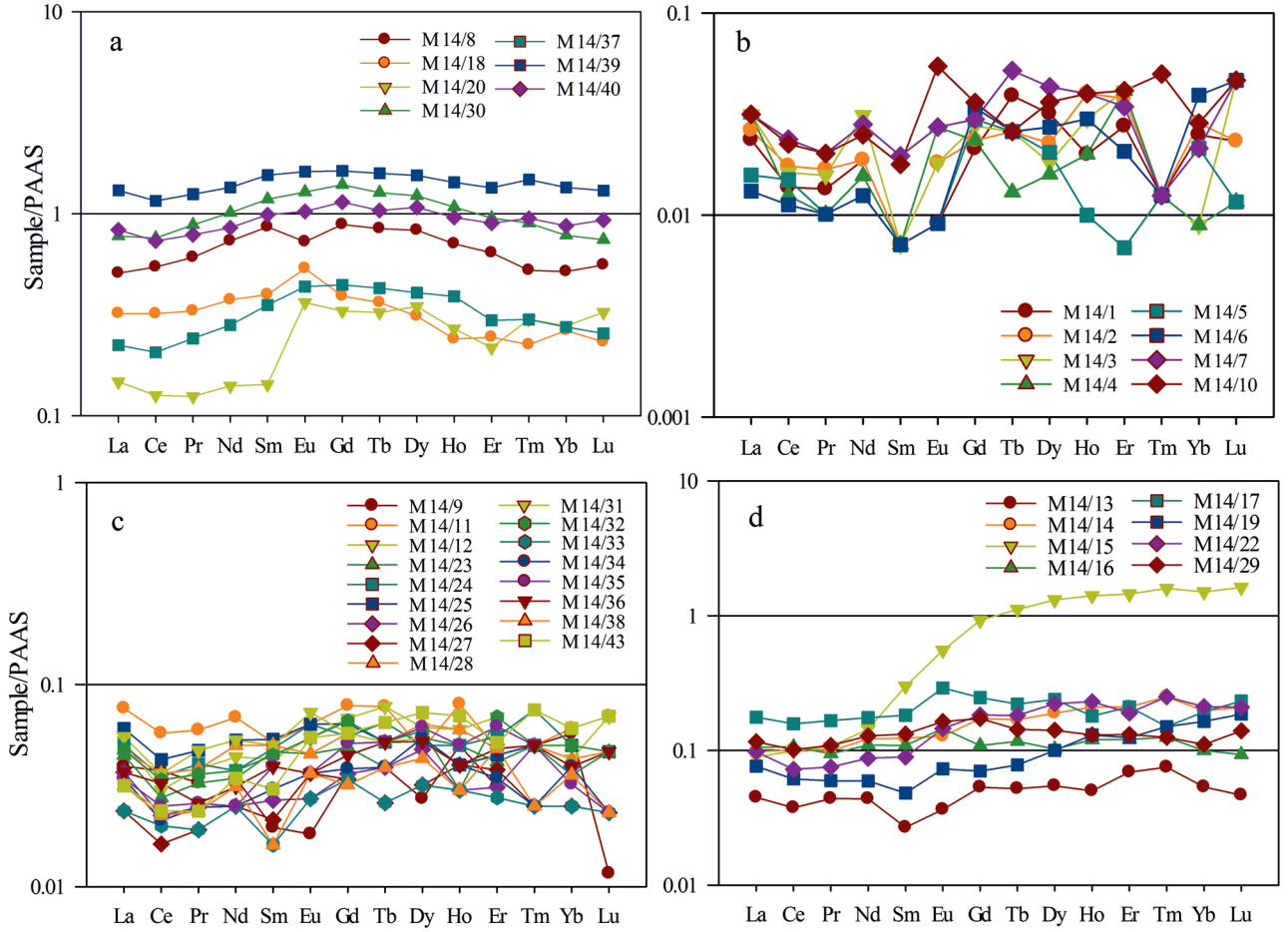

Fig. 5. PAAS-normalized REEs pattern of various rock types from Mannersdorf: **a** — clastic samples including lower siliciclastics and intercalated ones; **b** — pure limestone samples composed mainly of calcite; **c** — pure limestones composed of calcite and quartz; **d** — impure Leitha limestones with muscovite and clays.

Eu anomaly

Both pure and impure limestones from Mannersdorf have an average Eu anomaly value of 1.12 (0.68–2.15) which does not differ from the average value for the siliciclastics from the same locality which equals 1.13. The Eu anomaly from the Wöllersdorf limestones ranges from 0.58 to 1.1 with average of 0.9. Kummer samples including pure limestones, marly limestones and siliciclastics all have nearly the same Eu anomaly with an average value of 1.02, 1.03 and 1.05, respectively. Fertőrákos limestones have an Eu anomaly average of 1.09. The Eu anomaly of pure and impure limestones

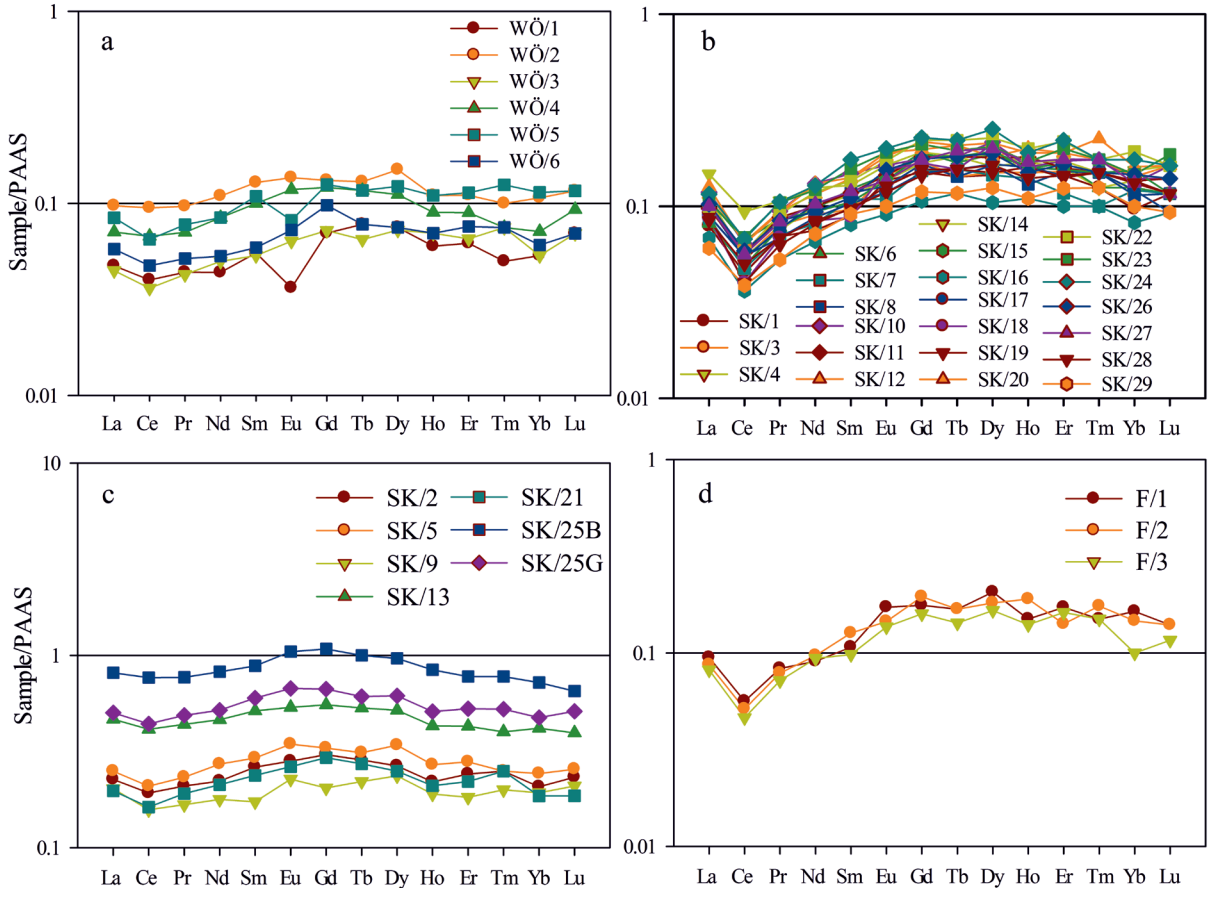

Fig. 6. PAAS-normalized REEs pattern of Leitha limestones: **a** — impure limestone samples from Wöllersdorf; **b** — pure limestone samples composed mainly of calcite at Kummer; **c** — impure samples from Kummer quarry where the lower ones are marly and the upper ones are siliciclastics; **d** — pure limestones from Fertőrákos locality.

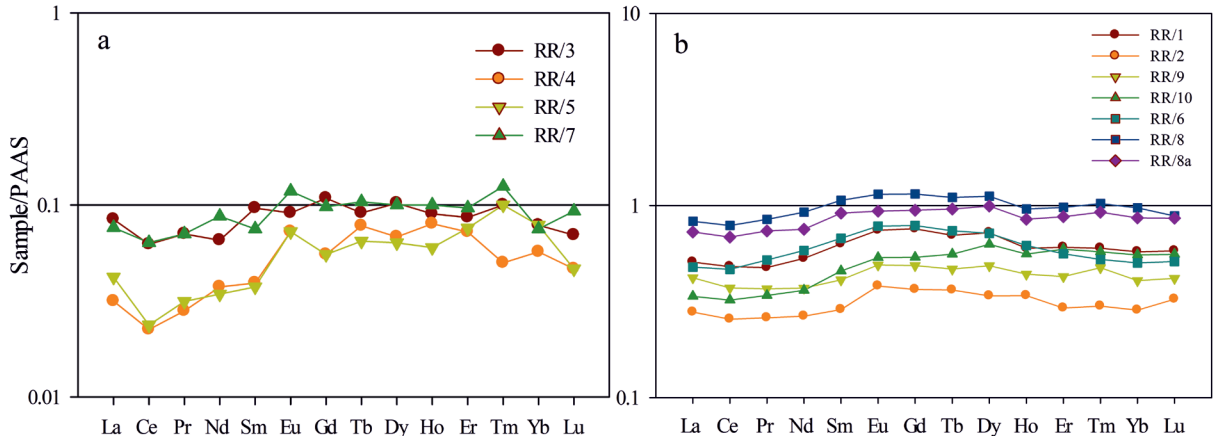

Fig. 7. PAAS-normalized REEs pattern of Leitha limestones: **a** — limestones from Rosenberg quarry including pure limestones (the lower two samples) and impure limestones (the upper two samples); **b** — siliciclastics samples from Rosenberg quarry.

from the Rosenberg quarry have averages of 1.6 and 1.13, respectively.

Y/Ho ratio

The average Y_{mol}/Ho_{mol} ratio of pure and impure limestones from Mannersdorf are approximately the same 34 and 33, respectively. In Wöllersdorf the limestone lithofacies containing dolomite has an average value of 31 which is lower than the average value in the lithofacies dominated by calcite with clays where it equals 33. In the Kummer pure limestones facies the average value is 39 and in the marly facies the ratio's average is 35. The limestones from Fertőrákos have exactly the similar ratios as the Kummer limestones. At Rosenberg the Y/Ho ratio averages 35 (31–45) in both pure and impure limestone facies.

Discussion

Factors controlling mineralogy

The Leitha limestones studied here have slightly different mineralogical compositions according to the sampling locality and its regional substratum geology. Samples from Mannersdorf and Wöllersdorf show the effect of intermittent siliciclastic input during limestone deposition as indicated by the presence of quartz and clay minerals, as well as the effect of diagenesis which led to the formation of dolomite. Various types of pure to impure limestones can be recognized in all the studied localities. Major impurities are quartz, clay minerals and other phyllosilicates, and feldspar (e.g. microcline), reworked and incorporated from adjacent basement complexes and derived from riverine input. The source of pyrite and barite in some samples may be related to the degradation of organic matter during the early stages of diagenesis which provides sulphur for the formation of such minerals in oxic to suboxic environments (Schieber 2011; Arndt et al. 2013).

In pure limestones from Kummer and Fertőrákos, the predominance of calcite and the sole abundance of clastic minerals (e.g., quartz and clay minerals) are also related to the role of erosion and reworking of pre-existing limestones in subaerial and shallow water conditions, as a result of reduced marine conditions and/or lowered sea level. This scenario is based on the deposition of sands, gravels and hydrodynamically controlled "detritic" Leitha limestones by Gilbert-type deltas in the Eisenstadt-Sopron Basin (Rostá 1993; Wiedl et al. 2014). Limestones from Rosenberg show detrital input signals especially in the impure limestone samples collected near the contact with underlying and overlying siliciclastics. Magmatic activity certainly played a role in affecting carbonate sedimentation in the studied area (Reuter et al. 2012). Mineralogically, dolomite formation in those limestones is related to the presence of intervening tuff layers, which are originally rich in Mg, acting as the primary source for dolomitization during early diagenesis.

Geochemistry

Major elements

Generally, CaO wt. % in the studied limestones varies in reverse relation to SiO_2 and Al_2O_3 which clearly indicates the effect of siliciclastic input and thus detrital dilution of carbonates during deposition. Al_2O_3 is used as a proxy for clay content in limestones (Nothdurft et al. 2004), and the average contents of 1.2 wt. % in impure limestones from Mannersdorf confirms their classification as shale-contaminated (average value for siliciclastic-contaminated carbonates is 0.42 wt. %, Veizer 1983). The same feature applies at Wöllersdorf with Al_2O_3 wt. % average of 0.63. On the other hand, pure limestones from Kummer and Fertőrákos do not show any significant siliciclastic contamination as indicated by Al_2O_3 contents below 0.37 wt. %. At Rosenberg, the two samples in contact with the underlying and overlying siliciclastics have Al_2O_3 contents of 0.7 and 0.8 wt. %, respectively, giving an indication of the contamination, while the two limestone samples further away from the contact and in the middle of the outcrop do not show a similar trend and can be classified as pure limestones with an Al_2O_3 wt. % average of 0.06.

Minor elements

The Leitha limestones exhibit a significant variation in Sr content, with a general increase towards the South of the studied Austrian basins (Fig. 8). Although Sr values are lower than the average global carbonate value (610 ppm, Mielke 1979), the Sr content in the different limestone facies at Mannersdorf is the highest among the various rock types in that area with an average of 231 ppm. The Sr/Ca ratio in carbonates is used as a proxy to track the variations in seawater Sr/Ca ratio (e.g., Ullmann et al. 2016) and the diagenesis (e.g., Ando et al. 2006). The Sr/Ca ratio with an average of 1/1845 in all the Leitha limestones samples is higher than the mean value given by Kulp et al. (1952) which should be less than 1/1000 in most types of limestone. The lowest content is recorded in Mannersdorf and Wöllersdorf with a maximum value of 352 ppm. The Sr is favoured to be incorporated into aragonite rather than calcite, but this Sr is lost during diagenetic transformation of the metastable aragonite into the stable calcite (Morse & Mackenzie 1990).

Two main causes of low Sr content in limestones from Mannersdorf and Wöllersdorf are proposed here. First, the main constituents of these limestones are corallincean red algae and foraminifers which are, mineralogically, high-Mg calcites (Scholle & Ulmer-Scholle 2003), more prone to low Sr contents. Second, the release of Sr to pore water during recrystallization of calcite (Baker & Bloomer 1988) reduces the Sr content of the deposits. Although, additional diagenetic studies should be carried out on these localities, we favour the second explanation because Leitha limestones with largely similar composition, for instance, from the Kummer quarry have higher Sr contents with slight upward increase due to diagenesis (Fig. 9).

The highest Sr content is recorded in samples from the Styrian basin (i.e. Rosenberg samples) not only in the limestones, but also in the siliciclastics except for two samples. This basin suffered volcanism with a wide spectrum of magmatic rocks during the Neogene to Quaternary evolution of the Carpathian-Pannonian region (Harangi et al. 2006; Seghedi & Downes 2011, Ali & Ntaflos 2013). Volcanic activity may have played a role in a higher primary Sr content of regional Badenian water masses, and thus may be preserved in limestones from the Rosenberg quarry. Scleractinian corals (e.g. *Porites* and *Tarbellastraea*, Riegl & Piller 2000) which are aragonitic (Scholle & Ulmer-Scholle 2003) could also account for parts of the higher Sr content.

REEs patterns

The total REEs contents in the pure and impure samples from Mannersdorf and impure samples from Wöllersdorf and their strong positive correlation with terrigenous proxies such as Al_2O_3 and Zr (Fig. 10) indicates the influence of the detrital input during sedimentation on the total REEs content. Zr is used as a terrigenous input proxy due to its resistance to weathering and alteration processes (Taylor & McLennan 1985) besides its low abundance in seawater (Boswell & Elderfield 1988) and the single valency state prevents the effect of the changing redox conditions during deposition (Calvert et al. 1996). The stratigraphic distribution of the REEs content at Mannersdorf does not show a clear relationship between the facies type and REEs concentration (Fig. 10). The PAAS normalized REEs patterns of all the Leitha limestones facies are flat in shape and display a non-seawater like pattern due to the effect of clay admixture. These flat patterns are similar to the patterns of shales which represent the original source of the REEs in the ocean (Elderfield 1988). There is no strong correlation between REEs content and detrital proxies such as Al_2O_3 and Zr (r=0.27 and −0.05, respectively) in Kummer pure limestones samples supporting the idea that these samples are not contaminated by siliciclastics and retain the (original) seawater signal better. The REEs contents in the studied facies types do not vary and have a limited range (Fig. 11). Also, REEs patterns in these samples and at Fertőrákos show seawater-like shale normalized REEs patterns, characterized by HREEs enrichment shown by the low $(La/Yb)_N$ ratio (average 0.74 for 23 samples), a negative Ce anomaly (average = 0.6) , and a high $(Y/Ho)_{mol}$ ratio (average = 39). These patterns are interpreted as preserving the primary sedimentary environmental signal of marine water under oxic conditions (Haley et al. 2004).

Both REEs pattern types exist in the Rosenberg samples, where impure samples in contact with the underlying and overlying siliciclastic and contaminated with shale have flat non-seawater like patterns with $(La/Yb)_N$ of average 1.04 (n=2), higher REEs content (average 13.4 ppm), lower $(Y/Ho)_{mol}$ ratio of average 31 and Ce anomaly of 0.84. On the other hand, the pure limestones samples are significantly different, displaying seawater-like patterns with HREEs enrichment with $(La/Yb)_N$ of average 0.54 (n=2), lower REEs content of average 6.1 ppm, higher $(Y/Ho)_{mol}$ ratio of average 39 and Ce anomaly of 0.7. The latter two samples suggest deposition of

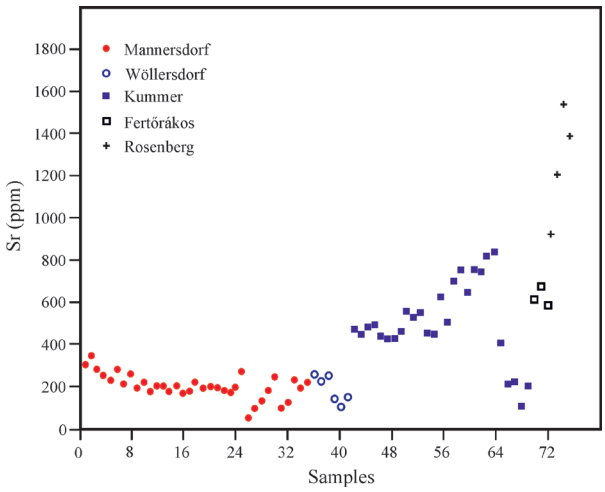

Fig. 8. Sr content of Leitha limestones from all localities, showing increasing values in Eisenstadt-Sopron (Kummer and Fertőrákos) and Styrian (Rosenberg) basins compared to the Vienna Basin (Mannersdorf and Wöllersdorf).

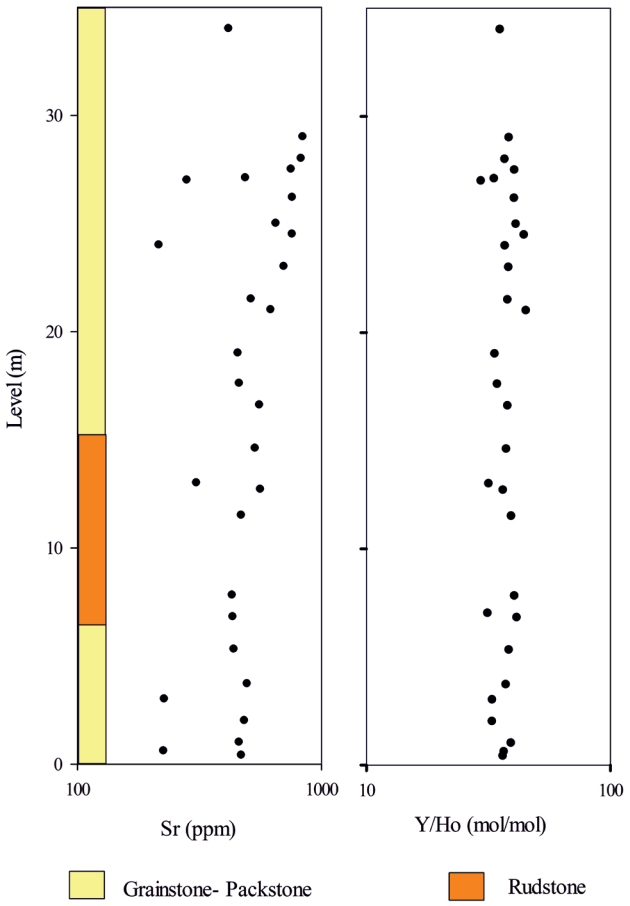

Fig. 9. Stratigraphic distributions of Sr content in the Kummer quarry with an increase upward, while Y/Ho ratio is almost the same in all samples (colours of facies after Schmid et al. 2001).

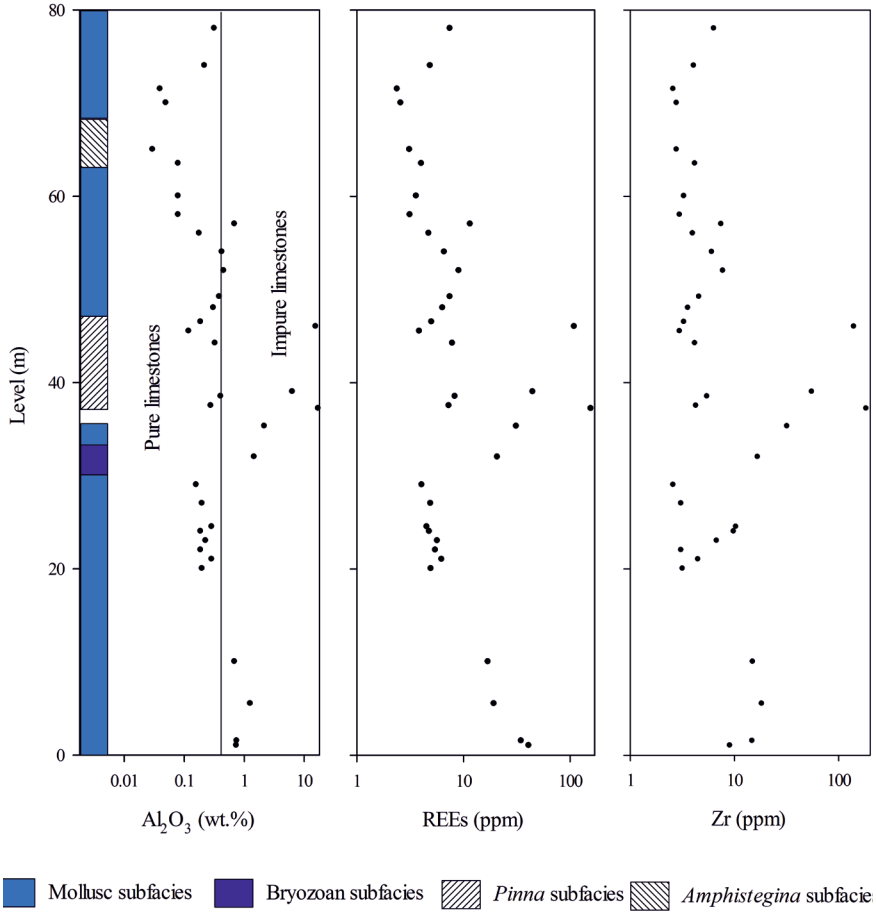

Fig. 10. Stratigraphic distributions of Al_2O_3, REEs and Zr at Mannersdorf with strong correlation between the three parameters (colours of facies after Wiedl et al. 2012).

the Rosenberg limestones under oxic conditions whereas more impure samples indicate a masking of the primary environmental (seawater) signal by siliciclastic contamination.

To test for the REEs elements pattern source three single-component samples were selected (cement, oyster shell, and pectinid shell) to be compared to the whole rock chemical analyses of the same parental samples. The cement fraction (sample M14/43) does not show a diverging total REEs content compared to the whole rock sample (5.28 vs. 5.73 ppm, respectively) but the Ce anomaly is different with a lower value of 0.62 in the cement fraction compared to 0.86. The REEs pattern in the cement fraction is more similar to the seawater-like pattern than the sample itself, with HREEs enrichment (i.e. $(La/Yb)_N$ value of 0.2), this ratio is 0.52 in the sample (Fig. 12a) and higher Y/Ho ratio of 27 and 23 for the whole sample. These relations give a hint of oxic marine conditions and cement precipitation from seawater trapped in pores during early diagenesis.

In samples from Kummer the total REEs content is lower in the biogenic fractions compared to the whole rock sample (3.22 and 2.78 ppm vs. 12.96 and 13.8 ppm in the whole rock samples). The REEs patterns in the whole rock samples are better defined than in the biogenic material (Fig. 12b) which can be explained by the lack of some elements such as Dy and Tm and the low elements contents of these fractions. The Ce anomaly is lower in the oyster shell (0.5 vs. 0.65 in the whole rock sample), a reverse situation to the pectinid shell where it is higher than the whole sample (0.59 vs. 0.52, respectively). Also, the Y/Ho ratio shows no clear trend from the shells versus the whole rock samples.

Ce anomaly

The Ce anomalies in limestones from Mannersdorf and Wöllersdorf are close to 1, and thus differ from seawater values (0.1–0.4). This can be explained by (1) the minor presence of clay minerals (from detrital input) in the pure and impure samples which is identified in all samples based on XRD analysis but to some extent by using SEM; (2) the release of LREEs due to the degradation of the organic matter including Ce in the few centimetres depth of the sediment column below the sea floor. Haley et al (2004) showed that in oxic environments the remineralization of organic coatings results in a balancing of the Ce anomaly to the value of the source material. Moreover, the presence of pyrite and barite supports such a conclusion by postulating that the organic matter was the source for sulphur (Schieber 2011; Arndt et al. 2013). The Ce anomaly record is different at Kummer and Fertőrákos, displaying considerably lower values (average 0.62) than at Mannersdorf and Wöllersdorf. This indicates primary seawater values and conforms to an interpretation of an oxic depositional environment, characterized by the lack of detectable detrital input which may have been removed during reworking and redeposition of the predominating detrital limestones from these localities. At Rosenberg, two ranges of Ce anomalies exist which indicate significant detrital input in impure limestones resulting in higher values whereas the lower values in pure limestones record primary oxic conditions.

Y/Ho ratio

The ratio of yttrium (Y) versus holmium (Ho) in the studied limestones samples is nearly similar in all the studied localities. The values are slightly higher in samples exhibiting low or no siliciclastic input (≥35 in relatively pure limestones) compared to samples with siliciclastic admixture (29–35 in impure limestones). The values indicate in general deposition

under oxic conditions. Due to the similarity in ionic radii of Y and Ho the expected oceanic distributions are closely similar (Zhang et al. 1994; Bau et al. 1995). Nevertheless, their different geochemical behaviour results in strong fractionation between the two elements. The former authors deduced that the Y/Ho ratios in seawater are approximately two times higher than the chondritic and shale ratios. The ratio is also affected by redox conditions where it decreases from 102 in oxic to 67 in anoxic waters as a consequence of preferential sorption of Ho with respect to Y on Fe- and Mn-oxyhydroxide particles that eventually dissolve under anoxic conditions (Bau et al. 1997). The fractionation takes place predominately in the ocean (Nozaki et al. 1997).

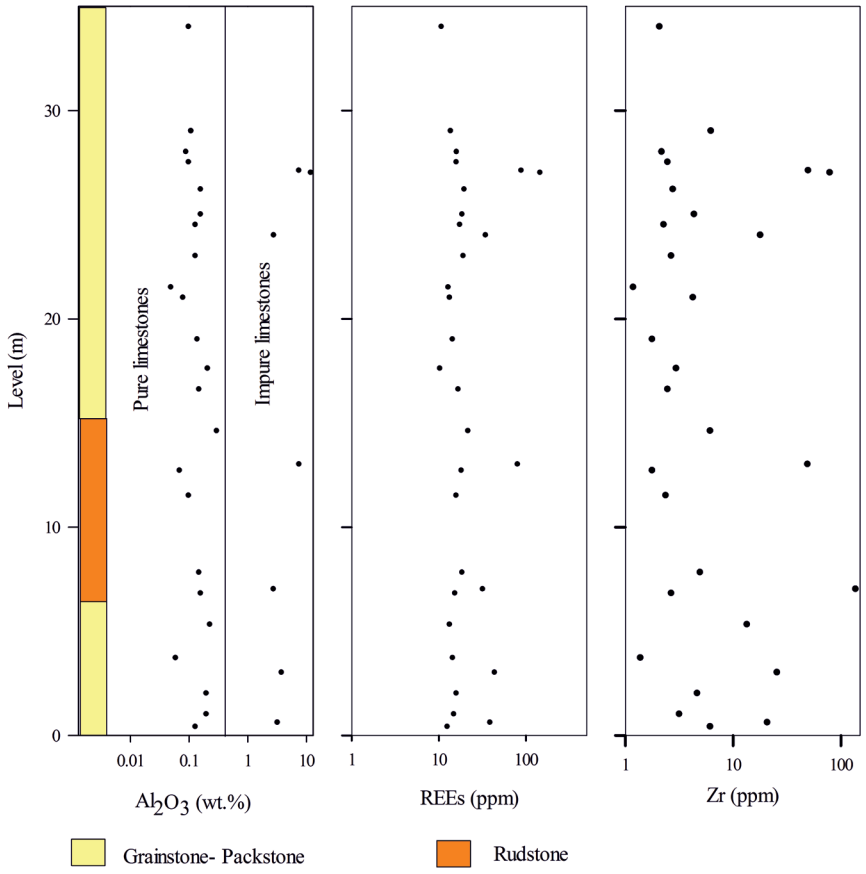

Fig. 11. Stratigraphic distributions of Al_2O_3, REEs and Zr at Kummer with weak positive correlation between REEs and Al_2O_3 and no correlation between REEs and Zr (colours of facies after Schmid et al. 2001).

Interpretation of controlling factors

The evidence derived from the mineralogical compositions and the above mentioned geochemical proxies account for the influence of several factors controlling the sediment geochemistry, notably the trace elements and RREs. In principle the following main factors govern the composition of the Miocene limestones: (1) detrital admixture from siliciclastics and volcaniclastics, (2) palaeoenvironmental signals from primary seawater composition and redox states, (3) diagenetic overprint. Detritally-contaminated limestones show clear deviations from the normal seawater conditions while the purer limestones point more clearly to the primary depositional environments if not strongly affected by diagenesis and later alteration.

Diagenetic evolution

There are significant differences in the diagenetic evolution between the studied localities. Chemical elements such as Sr, Na and Ba can be used as indices for the magnitude of diagenetic overprint, because these elements are generally incorporated during deposition and redistributed during diagenesis

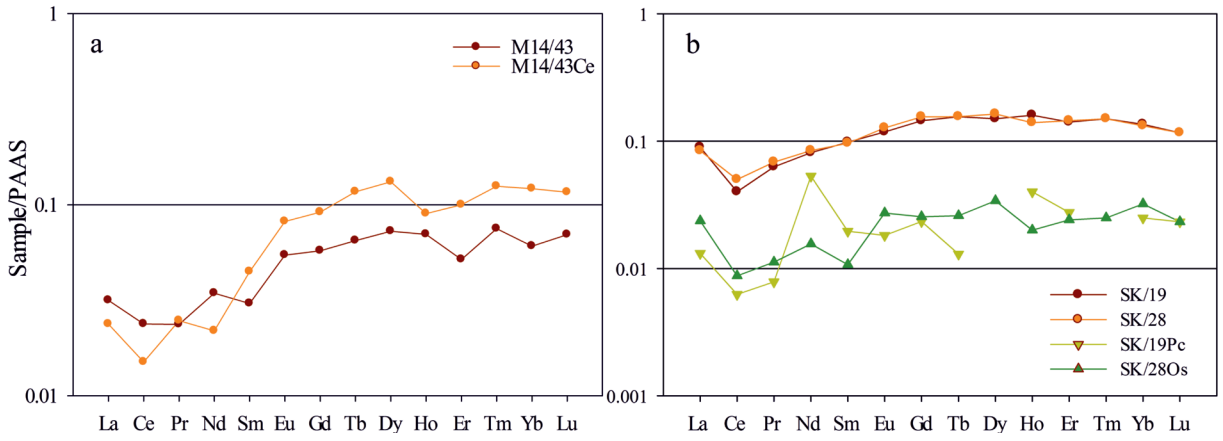

Fig. 12. a — REEs patterns of sample M14/43 from Mannersdorf compared to cement fraction (M14/43Ce) of the same sample, **b** — REEs patterns of the biotic fractions (oyster, pectinid shell) compared to the whole samples from Kummer.

(e.g., Land & Hoops 1973; Brand & Veizer 1980; Morrison & Brand 1986; Nothdurft et al. 2004; Webb et al. 2009). Here, the enrichment and/or depletion of these elements are used only to evaluate the relative degree of diagenesis in the studied limestones.

Intensive meteoric diagenesis, as expected and demonstrated for these carbonate platforms (Dullo 1983) leads to depletion in elements such as Sr, Na and Ba. The overall Sr content varies considerably, with low amounts in all limestone samples from Mannersdorf and Wöllersdorf (averages 221 ppm in Mannersdorf and 197 ppm in Wöllersdorf), and increasing from Kummer and Fertőrákos (average 570 ppm) to Rosenberg (average 1271 ppm) as shown in Figure 8. This trend indicates in general that Mannersdorf and Wöllersdorf limestones suffered more intensive diagenesis compared to the other localities. A similar trend in Na and Ba supports this idea. Mannersdorf and Wöllersdorf show the lowest values of these elements (Na not detected in most of the samples, average Ba of 15.6 ppm), followed Kummer and Fertőrákos (average 212.9 ppm Na, average 20.6 ppm Ba) and with the highest values at Rosenberg (average 315.3 ppm Na, average 43.5 ppm Ba). The above mentioned values for Na and Ba are derived only from pure limestone samples without visible contamination by detrital input to avoid mixing with the signal coming from clay minerals. The minimal diagenetic overprint on limestones from the Rosenberg quarry was previously also reported on the basis of stable isotopes studies on shell material (Bojar et al. 2004). REEs patterns are in accordance with this interpretation, indicating stronger diagenetic overprint influencing the palaeoenvironmental signal considerably at Mannersdorf and Wöllersdorf, whereas at Kummer and Rosenberg localities, the original seawater signal is largely preserved.

Provenance

Geological setting and relations to basement rocks at the studied localities gives the opportunity to evaluate the applicability of various elemental ratios to deduce the possible sources of siliciclastic input during shallow-water carbonate deposition. The distributions of immobile elements are used to interpret sediment sources and hinterland geology, for example, La and Th are enriched in acidic rocks, while Sc, Cr and Co are enriched in basic rocks (McLennan et al. 1983, 1990; Cullers 2000; Madhavaraju et al. 2010). The resulting elemental ratios are more affected by the composition of source rocks rather than the depositional environment (Cullers 1988, 1994). La/Sc, La/Co, Th/Sc, Th/Co and Th/Cr elemental ratios are used to evaluate and classify the detrital input sources. Elemental ratios of limestone samples from Mannersdorf and Kummer containing considerable amounts of detrital materials and siliciclastic samples from the former localities and Rosenberg are shown in Table 4. The Mannersdorf samples exhibit a wide range of elemental ratios indicating intermediate to silicic igneous rock sources, while the Kummer and Rosenberg samples plot in the range of silicic rocks (Figs. 13, 14). This conforms to the mainly silicic source material present in the Austroalpine basement units of the surrounding Alpine units (e.g., Schuster & Nowotny 2015), namely (meta) granites, gneisses and mica schists.

Palaeoenvironments

Considering pure (with respect to detrital contamination) and diagenetically relatively unaltered limestones, Ce and Eu anomalies can be used as proxies to infer palaeoenvironments, essentially indicating the redox state during limestone deposition. In addition, the Mn* values of the Leitha limestone samples are overall positive indicating deposition under oxic conditions. On the other hand, some siliciclastic samples from the three localities show negative Mn* values which point to (more) reducing depositional environments, in accordance with intermittently low-oxygen depositional sites and dysoxia events inferred for certain parts of the Leitha limestone platforms (Schmid et al. 2001).

Weathering

Weathering indices, related to source rock weathering, were evaluated here to test the applicability of these methods and to evaluate the transfer of the weathering signal from the source to the carbonates. The relative proportions of mobile element oxides (CaO, Na_2O and K_2O) to immobile element oxides

Table 4: Range of elemental ratios of Mannersdorf, Kummer and Rosenberg compared to felsic rocks, mafic rocks and PAAS.

	Mannersdorf impure Leitha limestones n=4	Mannersdorf siliciclastics n=8	Kummer marls n=4	Kummer siliciclastics n=3	Rosenberg siliciclastics n=7	Felsic rocks[a]	Mafic rocks[a]	PAAS[b]
La/Sc	0.49–4.4	0.62–3.21	2.87–3.85	2.93–2.95	2.13–3.86	2.5–16.3	0.43–0.86	2.4
La/Co	1.13–3.72	1.12–3.69	6.82–8.63	2.3–5.21	1.9–3.96	1.8–13.8	0.14–0.38	1.65
Th/Sc	0.07–1.2	0.35–1.82	0.87–1.1	0.86–1.03	0.53–1.23	0.84–20.5	0.05–0.22	0.90
Th/Co	0.17–0.94	0.27–1.91	2–4.2	0.78–1.82	0.54–1.61	0.67–19.4	0.04–1.4	0.63
Th/Cr	0.06–0.12	0.07–0.15	0.09–0.11	0.11	0.02–0.07	0.13–2.7	0.018–0.046	0.13
Cr/Th	8–17	7–186	9–11	9	15–47	4.0–15.0	25–500	7.53
Mn*	0.77–1.06	−0.72–0.21	0.92–1.47	−0.52–0.09	−0.32–0.84			
CIA	71.4–72.9	74.7–91.1	83.1–84	83.2–83.6	64.2–72.8			
CIW`	93.7–99.1	92.6–99.5	98.8–98.9	99	84.6–92.9			

[a]Cullers (1994, 2000); Cullers & Podkovyrov (2000); Cullers et al. (1988)
[b]Taylor & McLennan (1985)

(Al_2O_3) were used to determine the degree of chemical weathering, in our study related to weathering of the siliciclastic admixture in impure limestones; pure limestones cannot be used for these methods because of the low contents of the respective elements.

The Mannersdorf impure and Kummer marly limestones and siliciclastics show uniform, moderate to high degrees of chemical weathering with CIA values ranging from 71 to 91 (Table 4). Using the A-CN-K (Al_2O_3–CaO*+Na_2O–K_2O) ternary plot (Fig. 15), these values approach the muscovite and illite fields which have CIA values of 75 and 75 to 85, respectively (Nesbitt & Young 1982). Such values resulted from the transformation of feldspars (from felsic source rocks of the Austroalpine basement) into clay minerals along the transport path and finally deposited in limestones or as intercalated layers. In comparison, the Rosenberg samples show lower values (64–73, Fig. 15) with a low degree of chemical weathering indicating most probably the influence of the primarily volcano-siliciclastic input in the Styrian basin with short transport distance und thus minor weathering. The CIW` shows a similar trend to CIA among the studied samples (Table 4). In contrast to impure limestones, the application of the CIA index in pure limestones (i.e. low Al_2O_3 content below 0.42 wt. %, for example, in the Kummer limestones) proves impractical because the obtained values are attributed to low contents of both mobile and immobile oxides rather than a particular mineralogy.

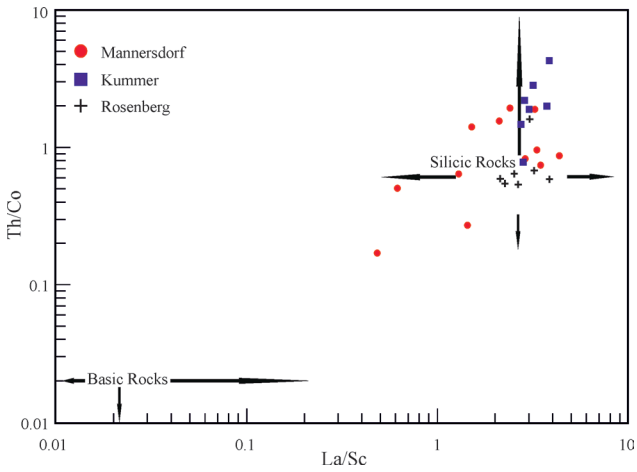

Fig. 13. Th/Co vs La/Sc plot of impure Leitha limestones samples containing detrital materials and siliciclastic samples from Mannersdorf (intermediate to silicic), Kummer and Rosenberg (silicic) quarries (after Cullers 2002).

Provenance versus palaeoenvironmental signals

Geochemical data from varying sites of Central Paratethys Middle Miocene carbonate platform limestones allow a testing of signals according to provenance and/or palaeo-environmental significance. Samples investigated range from pure limestones (Al_2O_3<0.42 wt. %, $CaCO_3$>99 wt. %) to impure limestones (Al_2O_3>0.42 wt. %, $CaCO_3$<80 wt. %, impurities from quartz, pyrite and evaporites) to siliciclastics (sands, clays) present as interlayers and below and/or above the limestones. Signals can thus be separated accordingly into those stemming from siliciclastic admixture, and so mainly influenced by provenance signals carried by the (minor) siliciclastic fraction, and palaeoenvironmental signals representing original sea-water composition — although this signal may also be indirectly influenced by the surrounding geology via dissolution and locally deviating water chemistry within the basins investigated.

As expected, the provenance signal is the main influence on various parameters as deduced from similar values going from impure to more pure limestones. Still, classical provenance indicators like immobile elemental ratios, CIA and CIW` are

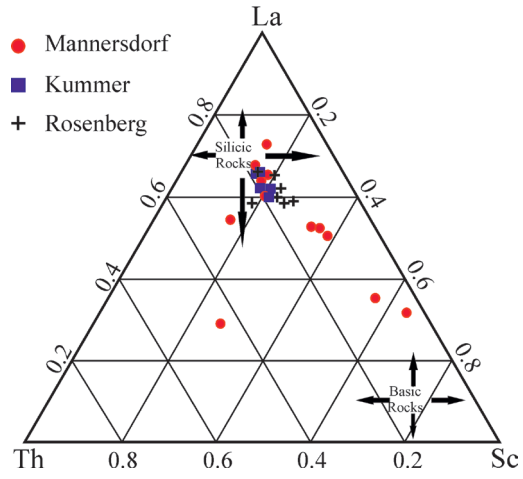

Fig. 14. La–Th–Sc ternary plot of impure Leitha limestones samples containing detrital materials and siliciclastic samples from Mannersdorf (intermediate to silicic), Kummer and Rosenberg (silicic) quarries (after Cullers 2002).

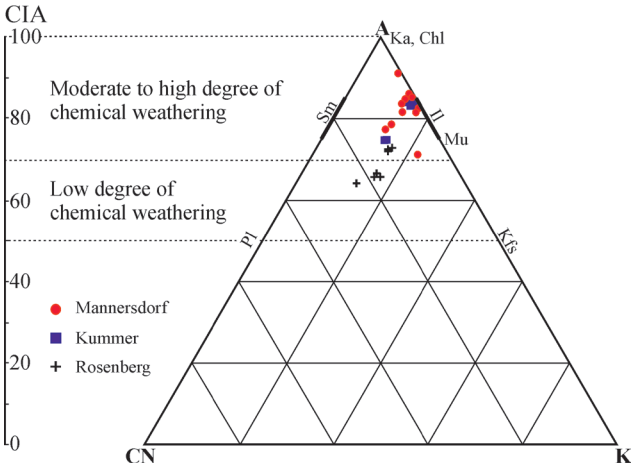

Fig. 15. A-CN-K ternary plot with the chemical index of alteration (CIA) of impure limestones, marls and siliciclastics of Mannersdorf, Kummer and Rosenberg quarries, mineral fields are represented by kaolinite (Ka), chlorite (Chl), illite (Il), muscovite (Mu), smectite (Sm), plagioclase (Pl) and K-feldspars (Kfs).

applicable and interpretable even in impure limestones such as those from Mannersdorf, which contain considerable amounts of Al_2O_3 up to 2.5 wt. % and marly samples from the Kummer quarry. The high values of the CIA indicate enhanced chemical weathering in the hinterland due to warm and humid palaeoclimate, and thus compatible with increased detrital input into the basins (Nesbitt & Young 1982; Zhao & Zheng 2014).

Furthermore, the stratigraphic evolution at Mannersdorf with a significant gradual decline in the detrital content (e.g., Al_2O_3, Fig. 10) upwards coincides with the regional palaeoclimatic changes in the Central Paratethys region in which a tropical (Wiedl et al. 2012) to warm-temperate climate (Mid-Miocene Climatic Optimum) was followed by gradual temperature decline (Ivanov et al. 2002; Hohenegger et al. 2009; Kováčová et al. 2009). Provenance signals are derived clearly as a function of the presence of detrital-siliciclastic material which, by itself, is also a function of weathering, palaeoclimate and palaeohydrology. The alternative explanation of enhanced detrital input due to tectonic subsidence and hinterland uplift is unlikely because of the significant decrease in tectonic activity during the middle to late Badenian (Lee & Wagreich 2017).

In contrast, only pure limestones with Al_2O_3 below 0.23 wt. % give reliable information about their specific depositional environment and environmental conditions in general. Thus, palaeo-environmental signals are relatively hard to decipher especially with increasing shale contamination into the limestones. However, some indices may still work in impure limestones with Mn*, Ce/Ce* and Eu/Eu* especially useful in the case of separating oxic from low-oxic/anoxic palaeoenvironments. All of these indices generally indicate deposition of the Leitha limestones under oxic conditions; only exceptional cases indicate low-oxic/anoxic conditions (e.g., negative Mn* values), also proven by faunal evidence such as the preservation of fish remains (Schmid et al. 2001). Other proxies show normal marine conditions as indicated by "normal" seawater values without further specifications.

Conclusions

The five studied Middle Miocene Leitha limestone occurrences exhibit various mineralogical, geochemical and environmental features. These features can be summarized as follows:

- The limestones were classified into pure limestones with Al_2O_3 content below 0.42 wt. % and the absence of clay minerals while impure limestones have higher Al_2O_3 and a detectable amount of clay minerals induced by the detrital input. Both limestone types exist in the studied localities with variable abundances.
- Limestones from Mannersdorf and Wöllersdorf (southern Vienna Basin) are influenced by detrital input during deposition which varies between intermediate to silicic sources in origin. This input appears in the mineralogy of the limestones which contain quartz and clay minerals in most of the samples. The input decreased with respect to age, probably due to the palaeoclimatic change to a slightly cooler climate during the Middle Miocene. Geochemically, the marine signal deduced by REEs patterns, Ce anomaly and Y/Ho ratio is masked by the detrital input in most of the samples. No clear relationship between facies types and geochemical characteristics can be deduced due to both significant detrital input and diagenetic influence.
- The Leitha limestones from Kummer and Fertőrákos (Eisenstadt–Sopron Basin) are purer with regard to the detrital input in which no clay minerals were detected. This criterion makes limestones from these localities excellent tracers for the primary depositional environments; at the same time it inhibits clear determination of provenance. REEs patterns, Ce anomaly and Y/Ho ratio indicate the deposition of limestones under oxic shallow marine conditions. The origin of the siliciclastics in the marly facies and in clay layers in Kummer quarry is from silicic igneous rocks. The palaeoenvironments of these siliciclastics were oxygen-deficient.
- The limestones from the Rosenberg quarry (Styrian Basin) were influenced by volcano-siliciclastic events during the Badenian, displayed by quartz, clay minerals, feldspars and dolomite especially in samples near the contact with the siliciclastics. The low degree of chemical weathering evidenced by low CIA values also assures the nearby and less altered volcano-siliciclastic source of the detrital input. The marine signal of these facies is not obvious due to this influence, while in the facies away from the contact with siliciclastics oxic shallow marine conditions represent the depositional environment. The source of the siliciclastics at Rosenberg is silicic igneous rocks for both underlying and overlaying ones.

In general, provenance signals are detectable going from (siliciclastic) sediments to impure limestones which contain Al_2O_3 down to 2.5 wt. %. The source rock signal is thus the main influence on limestone geochemistry in impure limestones, and classical provenance indicators like immobile elemental ratios, CIA and CIW` are applicable and interpretable even in slightly impure limestones. Proxies for reconstructing environmental conditions during deposition are mainly indices that may separate oxic from low-oxic/anoxic palaeoenvironments like Mn*, Ce/Ce* and Eu/Eu* which worked reliably going from impure to pure limestones.

Acknowledgements: We thank the quarry companies, especially Lafarge Zementwerke GmbH (former Lafarge-Perlmoser) for making available sampling in the active quarry sites, and for hospitality and support for the work. Thanks go to the Egyptian Cultural Affairs & Missions Sector for providing a PhD scholarship for the first author. Field work was partly financed by UNESCO-IUGS IGCP 609 and the Austrian Academy of Sciences. We also thank Shahid Iqbal and Wolfgang Knierzinger for assistance during field work, Sabine Hruby-Nichtenberger and Maria Meszar for sample preparation and lab work.

References

Ali Sh. & Ntaflos Th. 2013: Petrogenesis and mantle source characteristics of Quaternary alkaline mafic lavas in the western Carpathian–Pannonian Region, Styria, Austria. *Chem. Geol.* 337–338, 99–113.

Anderson P.E., Benton M.J., Trueman C.N., Paterson B.A. & Cuny G. 2007: Palaeoenvironments of vertebrates on the southern shore of Tethys: the nonmarine early cretaceous of Tunisia. *Palaeogeogr. Palaeoclimatol. Palaeoecol.* 243, 118–131.

Ando A., Kawahata H. & Kakegawa T. 2006: Sr/Ca ratios as indicators of varying modes of pelagic carbonate diagenesis in the ooze, chalk and limestone realms. *Sediment. Geol.* 191, 37–53.

Arndt S., Jørgensen B.B., LaRowe D.E., Middelburg J.J., Pancost R.D. & Regnier P. 2013: Quantifying the degradation of organic matter in marine sediments: A review and synthesis. *Earth Sci. Rev.* 123, 53–86.

Azmy K., Brand U., Sylvester P., Gleeson S.A., Logan A. & Bitner M.A. 2011: Biogenic and abiogenic low-Mg calcite (bLMC and aLMC): evaluation of seawater-REE composition, water masses and carbonate diagenesis. *Chem. Geol.* 280, 180–190.

Baker P.A. & Bloomer S.H. 1988: The origin of celestite in deep-sea carbonate sediments. *Geochim. Cosmochim. Acta* 52, 335–340.

Balogh K., Ebner F., Ravasz C., Herrmann P., Lobitzer H. & Solti G. 1994: K/Ar-Alter tertiärer Vulkanite der südöstlichen Steiermark und des südlichen Burgenlandes. In: Lobitzer H., Császár G. & Daurer A. (Eds.): Jubiläumsschrift 20 Jahre Geologische Zusammenarbeit Österreich–Ungarn. *Geol. Bundesanst.* Vienna, 55–72.

Bau M. 1991: Rare-earth element mobility during hydrothermal and metamorphic fluid- rock interaction and the significance of the oxidation state of europium. *Chem. Geol.* 93, 3, 219–230.

Bau M. & Dulski P. 1999: Comparing yttrium and rare earths in hydrothermal fluids from the Mid-Atlantic Ridge: implications for Y and REE behaviour during near-vent mixing and for the Y/Ho ratio of Proterozoic seawater. *Chem. Geol.* 155, 1, 77–90.

Bau M. & Möller P. 1992. Rare earth element fractionation in metamorphogenic hydrothermal calcite, magnesite and siderite. *Mineral. Petrol.* 45, 3–4, 231–246.

Bau M., Dulski P. & Möller P. 1995: Yttrium and holmium in South Pacific seawater: vertical distribution and possible fractionation mechanisms. *Chem. Erde* 55, l–15.

Bau M., Möller P. & Dulski P. 1997: Yttrium and lanthanides in eastern Mediterranean seawater and their fractionation during redox-cycling. *Mar. Chem.* 56, 123–131.

Bau M., Balan S., Schmidt K. & Koschinsky A. 2010: Rare earth elements in mussel shells of the Mytilidae family as tracers for hidden and fossil high-temperature hydrothermal systems. *Earth Planet. Sci. Lett.* 299, 310–316.

Bojar A-V., Hiden H., Fenninger A. & Neubauer F. 2004: Middle Miocene seasonal temperature changes in the Styrian basin, Austria, as recorded by the isotopic composition of pectinid and brachiopod shells. *Palaeogeogr. Palaeoclimatol. Palaeoecol.* 203, 95–105.

Boswell S.M. & Elderfield H. 1988: The determination of zirconium and hafnium in natural waters by isotope dilution mass spectrometry. *Mar. Chem.* 25, 197–210.

Brand U. & Veizer J. 1980: Chemical diagenesis of a multicomponent carbonate system-1: trace elements. *J. Sediment. Petrol.* 50, 1219–1236.

Calvert S.E., Burtin R.M. & Ingall E.D. 1996: Influence of water column anoxia and sediment supply on the burial and preservation of organic carbon in marine shales. *Geochim. Cosmochim. Acta* 60, 1577–1593.

Campbell A.C., Palmer M.R., Klinkhammer G.P., Bowers T.S., Edmond J.M., Lawrence J.R., Casey J.F., Thompson G., Humphris S., Rona R. & Karson J.A. 1988: Chemistry of hot springs on the Mid- Atlantic Ridge. *Nature* (London) 335, 514-519.

Chittleborough D.J. 1991: Indices of weathering for soils and palaeosols formed on silicate rocks. *Austr. J. Earth Sci.* 38, 115–120.

Craddock P.R., Bach W., Seewald J.S., Rouxel O.J., Reeves E. & Tivey M.K. 2010: Rare earth element abundances in hydrothermal fluids from the Manus Basin, Papua New Guinea: indicators of sub-seafloor hydrothermal processes in back-arc basins. *Geochim. Cosmochim. Acta* 74, 5494–5513.

Cullers R.L. 1988: Mineralogical and chemical changes of soil and stream sediment formed by intense weathering of the Danberg granite, Georgia, USA. *Lithos* 21, 301–314.

Cullers R.L. 1994: The controls on the major and trace element variation of shales, siltstones and sandstones of Pennsylvanian-Permian age from uplifted continental blocks in Colorado to platform sediment in Kansas, USA. *Geochim. Cosmochim. Acta* 58, 4955–4972.

Cullers R.L. 2000: The geochemistry of shales, siltstones and sandstones of Penn- sylvanianePermian age, Colorado, U.S.A.: implications for provenance and metamorphic studies. *Lithos* 51, 305–327.

Cullers R.L. 2002: Implications of elemental concentrations for provenance, redox conditions, and metamorphic studies of shales and limestones near Pueblo, CO, USA. *Chem. Geol.* 191, 305–327.

Cullers R.L. & Podkovyrov V.N. 2000: Geochemistry of the Mesoproterozoic Lakhanda shales in southeastern Yakutia, Russia: implications for mineralogical and provenance control, and recycling. *Precambrian Res.* 104, 77–93.

Cullers R.L., Basu A. & Suttner L. 1988: Geochemical signature of provenance in sand-size material in soils and stream sediments near the Tobacco Root batholith, Montana, USA. *Chem. Geol.* 70, 335–348.

de Baar H.J.W., Bacon M.P. & Brewer P.G. 1983: Rare-earth distributions with a positive Ce anomaly in the western North Atlantic Ocean. *Nature* 301, 324–327.

de Baar H.J.W., Bacon M.P., Brewer P.G. & Bruland K.W. 1985: Rare earth elements in the Pacific and Atlantic Oceans. *Geochim. Cosmochim. Acta* 49, 1943–1959.

Dubinin A.V. 2004: Geochemistry of rare earth elements in the ocean. *Lithol. Min. Resour.* 39, 289–307.

Dullo W.C. 1983: Fossildiagenese im miozänen Leitha-Kalk der Paratethys von Österreich: Ein Beispiel für Faunenverschiebung durch Diageneseunterschiede. *Facies* 8, 1–112.

Ebner F. & Sachsenhofer R.F. 1995: Palaeogeography, subsidence and thermal history of the Neogene Styrian basin (Pannonian basin system, Austria). *Tectonophysics* 242, 133–150.

Elderfield H. 1988: The oceanic chemistry of the rare-earth elements. *Philos. Trans. R. Soc. London,*325, 105–126.

Elderfield H. & Greaves M.J. 1982: The rare earth elements in seawater. *Nature* 296, 214–219.

Fenninger A. & Hubmann B. 1997: Palichnologie an der Karpatium/Badenium-Grenze des Steirischen Tertiärbeckens (Österreich). *Geol.-Paläontol. Mitt. Innsbruck,* 22, 71–83.

Haley B.A., Klinkhammer G.P. & McManus J. 2004: Rare earth elements in pore waters of marine sediments. *Geochim. Cosmochim. Acta* 68, 1265–1279.

Garbelli C., Angiolini L., Brand U., Shen S.Z., Jadoul F., Posenato R., Azmy K. & Cao C.Q. 2016: Neotethys seawater chemistry and temperature at the dawn of the end Permian mass extinction. *Gondwana Res.* 35, 272–285.

Handler R., Ebner F., Neubauer F., Hermann S., Bojar A.-V., Hermann S. 2006. 40Ar/39Ar dating of Miocene tuffs from Styrian part of the Pannonian Basin: an attempt to refine the basin stratigraphy. *Geol. Carpath.* 57, 483–494.

Haq B.U., Hardenbol J. & Vail P.R. 1987: Chronology of fluctuating sea levels since the Triassic. *Science* 235, 1156–1166.

Harangi S., Downes H. & Seghedi I. 2006: Tertiary-Quaternary subduction processes and related magmatism in the Alpine-Mediterranean region. In: Gee D.G. & Stephenson R.A. (Eds.): European Lithosphere Dynamics. *Geol. Soc. London Memoir* 32, 167–190.

Harnois L. 1988: The CIW index: a new chemical index of weathering. *Sediment. Geol.* 55, 319–322.

Harzhauser M. & Piller W.E. 2010: Molluscs as a major part of subtropical shallow-water carbonate production-an example from a Middle Miocene oolite shoal (Upper Serravallian, Austria). *Spec. Publ. Int. Ass. Sed.* 42, 185–200.

Hedberg H.D. 1976: International Stratigraphic Guide. *John Wiley,* New York, 1–200.

Hinkley T.K. & Tatsumoto M. 1987: Metals and isotopes in Juan de Fuca Ridge hydrothermal fluids and their associated solid materials. *J. Geophys. Res.* 92, 1943–1959.

Hohenegger J. & Wagreich M. 2012: Time calibration of sedimentary sections based on isolation cycles using combined cross-correlation: dating the gone Badenian stratotype (Middle Miocene, Paratethys, Vienna Basin, Austria) as an example. *Int. J. Earth Sci. (Geol. Rundsch.)* 101, 339–349.

Hohenegger J., Ćorić S., Khatun M., Pervesler P., Rögl F., Rupp C., Selge A., Uchman A. & Wagreich M. 2009: Cyclostratigraphic dating in the Lower Badenian (Middle Miocene) of the Vienna Basin (Austria): the Baden-Sooss core: *Int. J. Earth Sci. (Geol. Rundsch.)* 98, 915–930.

Hohenegger J., Ćorić S. & Wagreich M. 2014: Timing of the Middle Miocene Badenian Stage of the Central Paratethys. *Geol. Carpath.* 65, 1, 55–66.

Hongo Y. & Nozaki Y. 2001: Rare earth element geochemistry of hydrothermal deposits and Calyptogena shell from the Iheya Ridge vent field, Okinawa Trough. *Geochem. J.* 35,5, 347–354.

Ivanov D., Ashraf A.R., Mosbrugger V. & Palamarev E. 2002: Palynological evidence for Miocene climate change in the Forecarpathian Basin (Central Paratethys NW Bulgaria). *Palaeogeogr. Palaeoclimatol. Palaeoecol.* 178, 19–37.

Johannesson K.H., Telfeyan K., Chevis D.A., Rosenheim B.E. & Leybourne M.I. 2014: Rare earth elements in stromatolites-1. Evidence that modern terrestrial stromatolites fractionate rare earth elements during incorporation from ambient waters. In: Evolution of Archean Crust and Early Life. *Springer Netherlands,* 385–411.

Kim J.H., Torres M.E., Haley B.A., Kastner M., Pohlman J.W., Riedel M. & Lee Y.J. 2012: The effect of diagenesis and fluid migration on rare earth element distribution in pore fluids of the northern Cascadia accretionary margin. *Chem. Geol.* 291, 152–165.

Kocsis L., Trueman C.N. & Palmer M.R. 2010: Protracted diagenetic alteration of REE contents in fossil bioapatites: direct evidence from Lu–Hf isotope systematics. *Geochim. Cosmochim. Acta* 74, 21, 6077–6092.

Kováč M., Andreyeva-Grigorovich A., Bajraktarević Z., Brzobohatý R., Filipescu S., Fodor L., Harzhauser M., Nagymarosy A., Oszczypko N., Pavelić D., Rögl F., Saftić, B., Sliva L. & Studencka B. 2007: Badenian evolution of the Central Paratethys Sea: paleogeography, climate and eustatic sea level changes. *Geol. Carpath.* 58, 579–606.

Kováčová P., Emmanuel L., Hudáčkova N. & Renard N. 2009: Central Paratethys paleoenvironment during the Badenian (Middle Miocene): evidence from foraminifera and stable isotope (∂^{13}C and ∂^{18}O) study in the Vienna Basin (Slovakia). *Int. J. Earth Sci. (Geol. Rundsch.)* 98, 1109–1127.

Kröll A. 1988: Reliefkarte des prätertiären/Untergrundes. In: Kröll A., Flügel H.W., Seiberl W., Weber F., Walach G. & Zych D. (Eds.): Erläuterungen zu den Karten über den prätertiären Untergrund des Steirischen Beckens und der Südburgenländischen Schwelle. *Geologische Bundesanstalt*, Vienna, 16–20.

Kulp J.L., Turckian K. & Boyd D.W. 1952: Sr content of limestones and fossils. *Geol. Soc. Am. Bull.* 63, 701–716.

Land L.S. & Hoops G.K. 1973: Sodium in carbonate sediments and rocks: a possible index to the salinity of diagenetic solutions. *J. Sediment. Petrol.* 43, 614–617.

Lankreijer A., Kováč M., Cloetingh S., Pitoňák P., Hlôška M. & Biermann C. 1995: Quantitative subsidence analysis and forward modelling of the Vienna and Danube basins: thin-skinned versus thick skinned extension. *Tectonophysics* 252, 433–451.

Laskarev V.N. 1924: Sur les equivalentes du Sarmatien supérieur en Serbie. *Recueil de traveaux ofert a M. Jovan Cvijic par ses amis et collaborateurs,* 73–85.

Lee E.Y. & Wagreich M. 2017: Polyphase tectonic subsidence evolution of the Vienna Basin inferred from quantitative subsidence analysis of the northern and central parts. *Int. J. Earth Sci.* 106, 687–705.

Madhavaraju J., González-León C.M., Lee Yong Il., Armstrong-Altrin J.S. & Reyes-Campero L.M. 2010: Geochemistry of the Mural Formation (Aptian–Albian) of the Bisbee Group, Northern Sonora, Mexico. *Cretaceous Res.* 31, 400–414.

McLennan S.M., Taylor S.R. & Eriksson K.A. 1983: Geochemistry of Archean shales from the Pilbara Supergroup, Western Australia. *Geochim. Cosmochim. Acta* 47, 1211–1222.

McLennan S.M., Taylor S.R., McCulloch M.T. & Maynard J.B. 1990: Geochemistry and Nd-Sr isotopic composition of deep-sea turbidites: Crustal evolution and plate tectonic associations. *Geochim. Cosmochim. Acta* 54, 2014–2050.

McLennan S.M., Hemming S., McDaniel D.K. & Hanson G.M. 1993: Geochemical approaches to sedimentation, provenance, and tectonics. In: Johnsson M.J. & Basu A. (Eds.): Processes Controlling the Composition of Clastic Sediments. *Geol. Soc. Am., Spec. Pap.* 284, 21–40.

Michard A., Albarède F., Michard G., Minster J.F. & Charlou J.L. 1983: Rare earth elements and uranium in high-temperature solutions from East Pacific Rise hydrolhermal vent field (13º N). *Nature* (London), 303, 795–797.

Mielke J.E. 1979: Composition of the Earth's crust and distribution of the elements. In: Siegel F.R. (Ed.), Review of Research on Modern Problems in Geochemistry. *UNESCO Report*, Paris, 13–37.

Morrison J.O. & Brand U. 1986: Geochemistry of recent marine invertebrates. *Geoscience Canada,* 13, 237–254.

Morse J.W. & Mackenzie F.T. 1990: Geochemistry of Sedimentary Carbonates. *Elsevier,* Amsterdam, 1–707.

Nesbitt H.W. & Young G.M. 1982: Early Proterozoic climates and plate motions inferred from major element chemistry of lutites. *Nature* 299, 715–717.

Neuhuber S., Gier S., Hohenegger J., Wolfgring E., Spötl C., Strauss P. & Wagreich M. 2016: Palaeoenvironmental changes in the northwestern Tethys during the Late Campanian Radotruncana calcarata Zone: Implications from stable isotopes and geochemistry. *Chem. Geol.* 420, 280–296.

Nothdurft L.D., Webb G.E. & Kamber B.S. 2004: Rare earth element geochemistry of Late Devonian reefal carbonates, Canning Basin, Western Australia: confirmation of seawater REE proxy in ancient limestones. *Geochim. Cosmochim. Acta* 68, 263–283.

Nozaki Y. 2001: Rare earth elements and their isotopes. *Encycl. Ocean Sci.* 4, 2354–2366.

Nozaki Y., Zhang J. & Amakawa H 1997: The fractionation between Y and Ho in the marine environment. *Earth Planet. Sci. Lett.* 148, 329–340.

Olivarez A.M. & Owen R.M. 1991: The europium anomaly of sweater: implications for fluvial versus hydrothermal REE inputs to the oceans. *Chem. Geol.* 92, 317–328.

Papp A., Cicha I., Senes J. & Steininger F. 1978: M4-Badenien (Moravien, Wielicien, Kosovien). Chronostratigraphie und Neostratotypen. Miozän der Zentralen Paratethys. *Slowakische Akademie der Wissenschaften,* Bratislava, 1–594.

Piepgras D.J. & Jacobsen S.B. 1992: The behavior of rare earth elements in seawater: Precise determination of variations in the North Pacific water column. *Geochim. Cosmochim. Acta* 56, 1851–1862.

Piller W.E. & Kleemann K. 1991: Middle Miocene Reefs and related facies in eastern Austria. 1) Vienna Basin: VI International Symposium on Fossil Cnidaria including Archaeocyatha and Porifera. *Excursion Guidebook, Excursion B4*, 1–28.

Piller W.E., Decker K. & Haas M 1996: Sedimentologie und Beckendynamik des Wiener Beckens: Sediment 96, 11. Sedimentologentreffen, Exkursion guide, *Geol. Bundesanst.,* Wien, 1–41.

Piller W.E., Summesberger H., Draxler I., Harzhauser M. & Mandic O. 1997: Meso- to Cenozoic tropical/subtropical climates — Selected examples from the Northern Calcareous Alps and the Vienna Basin. In: Kollmann H.A. & Hubmann B. (Eds.) Excursion Guides, *Second European Paleontological Congress*, Climates: Past, Present and Future, Wien, 70–111.

Piller W.E., Harzhauser M. & Mandic O. 2007: Miocene Central Paratethys stratigraphy-current status and future directions. *Stratigraphy* 4, 151–168.

Piper D.Z. 1974: Rare earth elements in the sedimentary cycle: a summary. *Chem. Geol.* 14, 285–304.

Reuter M., Piller W.E. & Erhart C. 2012: A Middle Miocene carbonate platform under silici-volcaniclastic sedimentation stress (Leitha Limestone, Styrian Basin, Austria)- Depositional environments, sedimentary evolution and palaeoecology: *Palaeogeogr. Paleoclimatol. Paleoecol.* 350–352, 198–211.

Riegl B. & Piller W.E. 2000: Biostromal coral facies - a Miocene example from the Leitha Limestone (Austria) and its actualistic interpretation. *Palaios* 15, 399–413.

Rohatsch A. 2005: Neogene Bau- und Dekorgesteine Niederösterreichs und des Burgenlandes. *Mitteilungen IAG BOKU*, 9–56.

Rostá E. 1993: Gilbert-type delta in the Sarmatian-Pannonian sediments, Sopron, NW Hungary. *Földtani Közlöny* 123, 2, 167–193.

Royden L.H. 1985: The Vienna Basin: a thin-skinned pull-apart basin. In: Biddle K.T. & Christie-Blick N. (Eds) Strike-Slip deformation, basin formation, and sedimentation. *SEPM Spec. Publ.* 37, 319–338

Salvador A. 1994: International stratigraphic guide. *International Union of Geological Sciences and The Geological Society of America,* 1–214.

Schieber J. 2011: Marcasite in black shales- a mineral proxy for oxygenated bottom waters and intermittent oxidation of carbonaceous muds. *J. Sediment. Res.* 81, 447–458.

Schmid H.P., Harzhauser M. & Kroh A. 2001: Hypoxic events on a Middle Miocene carbonate platform of the Central Paratethys (Austria, Badenian, 14 Ma). *Ann. Naturhist. Mus. Wien* 102, 1–50.

Schmidt K., Garbe-Schönberg D., Bau M. & Koschinsky A. 2010: Rare earth element distribution in >400 ºC hot hydrothermal fluids from 5º S, MAR: the role of anhydrite in controlling highly variable distribution patterns. *Geochim. Cosmochim. Acta* 74, 4058–4077.

Scholle P.A. & Ulmer-Scholle D.S. 2003: A Color Guide to the Petrography of Carbonate Rocks. *AAPG Memoir* 77, 1–474.

Schreilechner M.G. & Sachsenhofer R.F. 2007: High resolution sequence stratigraphy in the eastern Styrian Basin (Miocene, Austria). *Austrian J. Earth Sci.* 100, 164–184.

Schuster R. & Nowotny A. 2015: Die Einheiten des Ostalpinen Kristallins auf den Kartenblättern GK50 Blatt 103 Kindberg und 135 Birkfeld. *Arbeitstagung der Geologischen Bundesanstalt Mitterdorf im Mürztal,* 10–37.

Seghedi I. & Downes H. 2011: Geochemistry and tectonic development of Cenozoic magmatism in the Carpathian-Pannonian region. *Gondwana Res.* 20, 655–672

Slapansky P., Belocky R., Fröschl H., Hradecký P. & Spindler P. 1999: Petrography, Geochemie und geotektonische Einstufung des miozänen Vulkanismus im Steirischen Becken (Österreich). *Abhandlungen der Geologischen Bundesanstalt* 56, 419–434.

Steininger F.F. & Piller W.E. 1999: Empfehlungen (Richtlinien) zur Handhabung der stratigraphischen Nomenklatur. *Courier Forschungsinstitut Senckenberg* 209, 1–19.

Strauss P., Harzhauser M., Hinsch R. & Wagreich M. 2006: Sequence stratigraphy in a classic pull-apart basin (Neogene, Vienna Basin). A 3D seismic based integrated approach. *Geol. Carpath.* 57, 185–197.

Suess E. 1860: Erhaltung von Fossilresten im Leithakalk. *Verhandlungen der Geologischen Reichsanstalt,* 1860, 1–9.

Taylor S.R. & McLennan S.M. 1985: The continental crust, its composition and evolution. *Blackwell, 1–328.*

Tollmann A. 1985: Geologie von Österreich. Band II. *Außerzentralalpiner Anteil: Deuticke,* Wien, 1–710.

Ullmann C.V., Campbell H.J., Frei R. & Korte C. 2016: Oxygen and carbon isotope and Sr/Ca signatures of high-latitude Permian to Jurassic calcite fossils from New Zealand and New Caledonia. *Gondwana Res.* 38, 60–73.

Veizer J. 1983: Trace elements and isotopes in sedimentary carbonates. In: Reeder RJ (ed.): Carbonates: Mineralogy and Chemistry. *Mineral. Soc. Am.* 11, 265–299.

Wagreich M. & Schmid H.P. 2002: Backstripping dip-slip fault histories: apparent slip rates for the Miocene of the Vienna Basin. *Terra Nova* 14, 163–168.

Webb G.E., Nothdurft L.D., Kamber B.S., Kloprogge J.T. & Zhao J. 2009: Rare earth element geochemistry of scleractinian coral skeleton during meteoric diagenesis: a sequence through neomorphism of aragonite to calcite. *Sedimentology* 56, 1433–1463.

Wedepohl K.H. 1978: Manganese: abundance in common sediments and sedimentary rocks. Handbook of Geochemistry. *Springer*, Berlin, 1-17.

Wessely G. 1983: Zur Geologie und Hydrodynamik im südlichen-Wiener Becken und seiner Randzone. *Mitt. Geol. Ges. Wien* 76, 27–68.

Wessely G. 2006: Geologie der Österreichischen Bundesländer — Niederösterreich. *Geologische Bundesanstalt,* Wien, 1–416.

Wiedl T., Harzhauser M. & Piller W.E. 2012: Facies and synsedimentary tectonics on a Badenian carbonate platform in the southern Vienna Basin (Austria, Central Paratethys). *Facies* 58, 523–548

Wiedl T., Harzhauser M., Kroh A., Ćorić S. & Piller W.E. 2013: Ecospace variability along a carbonate platform at the northern boundary of the Miocene reef belt (Upper Langhian, Austria). *Palaeogeogr. Palaeoclimatol. Palaeoecol.* 370, 232–246.

Wiedl T., Harzhauser M., Kroh A., Ćorić S. & Piller W.E. 2014: From biologically to hydrodynamically controlled carbonate production by tectonically induced paleogeographic rearrangement (Middle Miocene, Pannonian Basin). *Facies* 60, 865–881.

Zhang J., Amakawa H. & Nozaki Y. 1994: The comparative behaviors of yttrium and lanthanides in the seawater of the North Pacific. *Geophys. Res. Lett.* 21, 2677–2680.

Zhao M.Y. & Zheng Y.F. 2014: Marine carbonate records of terrigenous input into Paleotethyan seawater: Geochemical constraints from Carboniferous limestones. *Geochim. Cosmochim. Acta* 141, 508–531.